Verdazyl-based Bent-Core Liquid Crystals

by

Jason Gerding

Thesis

Submitted to the Faculty of the

Graduate School of Vanderbilt University

in partial fulfillment of the requirements

for the degree of

MASTER OF SCIENCE

in

Chemistry

May 2015

Nashville, Tennessee

Approved:

Piotr Kaszynski, PhD

Carmelo Rizzo, PhD

ACKNOWLEDGEMENTS

This work was financially supported by the D Stanley and Anne T Tarbell Endowment fund, the Vanderbilt Chemistry Department, and a grant from the National Science Foundation. I also want to express my gratitude to my wife, Francesca, for her encouragement through these years. My professors have also been a great source of learning, professional development and inspiration. Lastly, I also thank my labmates for their insight and support during my graduate career.

TABLE OF CONTENTS

PAGE

LIST OF TABLES

TABLE **PAGE**

LIST OF FIGURES

FIGURES **PAGE**

LIST OF SCHEMES

SCHEMES **PAGE**

Chapter 1: Introduction & Background

Liquid Crystals

The three common states of matter, solid, liquid, gas, have been well known since antiquity. A fourth, the liquid crystal, has been relatively newly discovered.[1] This state is characteristic in that it is a combination of long range order as in solid crystals, and yet it retains mobility like a liquid.[2] Unlike a crystal that loses both positional and orientational order upon transition from solid to an ordinary liquid, a liquid crystal will retain some or all orientational order while losing all positional order, allowing it to flow as a liquid. The retention of orientational order prevents the axes of the molecules from tumbling in any indiscriminate direction as they do in an ordinary liquid. This leads to anisotropy of the material as its flow is direction dependent, which can be influenced by external stimuli, and is therefore interesting to materials research.[2]

Liquid crystals are typically rod-like calamitics or disk-shaped discotics. The common structure of calamitic liquid crystals is shown in Figure 1. Here we see two rigid core units (ovals) connected by a linking group (L) in an antipodal relation to the core units, attached to alkyl chains through connecting groups (C).

Figure 1. Schematic diagram of a typical calamitic liquid crystal.

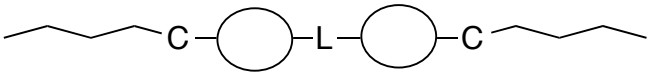

These calamitic molecules are designed to have an anisotropic shape which gives an axially parallel organization of the rigid units (i.e., orientational order), and the flexible chains allow for

mobility that inhibits crystallization. This parallel alignment results from the minimization of volume and the segregation of incompatible parts, for example flexible alkyl chains with rigid aromatic units.[3]

Depending on the degree of orientational order maintained, the liquid crystalline molecules are able to self-organize in numerous structures. Nematic, smectic, and columnar organizations result from the degrees of freedom retained or lost from the solid crystal state.[4] Nematic, being the least viscous and the simplest, has three degrees of freedom, followed by smectic with two, and columnar with one degree of freedom.[2] Examples of some of these supramolecular structures are shown in Figure 2. The loss of one degree of freedom from nematic to smectic means that a nematic phase has a non-uniform arrangement of molecules, whereas the molecules arrange in layers in smectic organization.

Fig 2. Graphical representation of nematic (N) and smectic (Sm) mesophases. SmC is a tilted version of SmA. Synclinic (SmC_s) and antisynclinic (SmC_a) versions are also shown. This helical superstructure shown is termed B4. Adapted from Ref. 3.

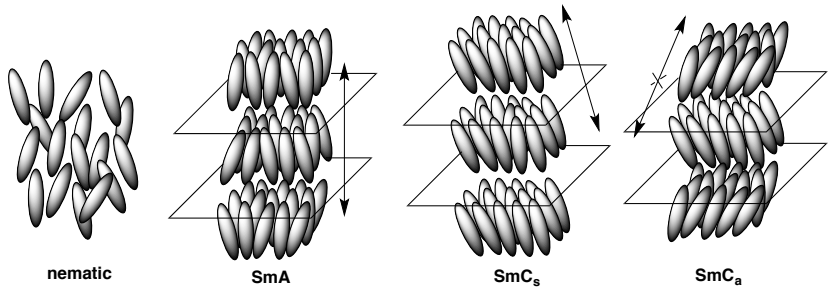

Both chemical structure and conformational dynamics determine average molecular shape. For example, calamitics, as mentioned above, obtain an average cylindrical shape by rapidly rotate around the long axis.[4] These rods may align perpendicular or tilted relative to the plane between layers. An example of the former arrangement is termed smectic A (SmA), whereas the latter is termed smectic C (SmC). In addition to being tilted relative to the layer

plane, the orientation of the tilted molecules between layers is designated as synclinic (SmC_s) when the molecules point in the same direction, or anticlinic (SmC_a), when the layers are pointed in opposite direction (Figure 2). Altering chemical structure by introducing molecular chirality can lead to helical phases and tilted phases (Figure 2). These are important considerations when designing liquid crystals and their elastic, electric, magnetic, and optic properties.[2]

Bent-Core Mesogens and Their Properties

In addition to the three types of liquid crystalline structures mentioned, SmA, SmC_s, and SmC_a, there is also a banana-shaped mesophase derived from a bent-core molecular structure. The difference comes from an angular rigid core rather than an antipodal central core unit as in calamitics. Although it is often the difference of only one position (e.g., 1,3- instead of 1,4-disubstitution), the consequences are apparent. The bent nature of the mesogen may lead to a macroscopic polar order.[3] This has significant effects on the formation and structure of liquid crystalline phases. As in all systems in nature, a gradient is fiercely resisted; therefore macroscopic polar domains are unstable and thus re-organize in a fluid environment to find zero net polarity. Thus, a mesogen may exist as a nematic, SmA, SmC_s, and SmC_a, but in such a manner where the bent core mesogens align in an anti-parallel relation to each other and so giving rise to a plethora of mesophases. During *layer modulation*, smectic layers avoid bulk polarization by the 2-dimentional rearrangement of the layers, thus giving either an intercalated or a columnar organization, where the stacking of such layers produces 3-dimentional columns in the latter (Figure 3a,b,c).[4] There is also *layer correlation* where distinct adjacent layers have their polar directions lie antiparallel (Figure 3d).[3] *Helix formations* may also arise where the distinct layers twist at a uniform angle (Figure 3e,f).[5]

Figure 3. Graphical demonstrations of potential banana-phase superstructures.[Reproduced from ref. 3 with permission from The Royal Society of Chemistry.]

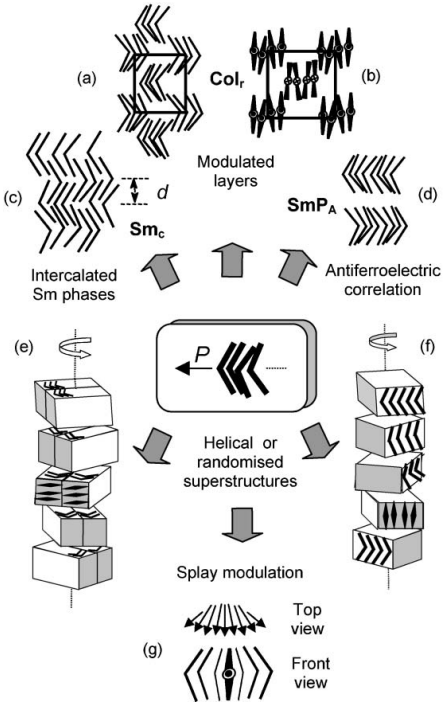

The bent shape of these liquid crystals gives various morphological possibilities. Although in the ground state the net polarity of the material is zero, individual layers may exhibit polar directionality. Polarity is determined by the direction of the bent core unit in relation to the aliphatic chains (Figure 4).

Figure 4. Layer modulation of bent-core molecules. Here we see two layers of bent-core molecules in relation to one another with the vertices signifying the rigid core unit and the ends representing the aliphatic tails. [Adapted from ref. 3.]

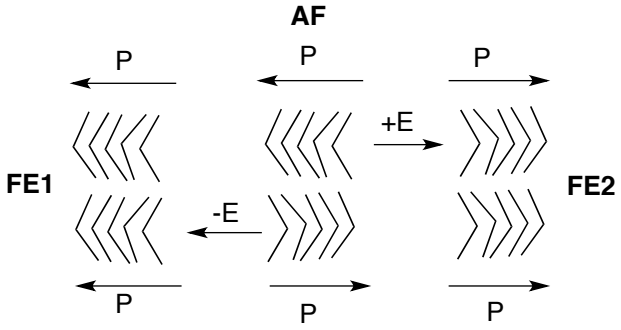

This shape anisotropy is significant in comparison to calamitic liquid crystals when subjected to external stimuli. As compared to the overall cylindrical shape of calamitics previously mentioned, the polar direction of banana-shaped mesogens will change from the ground state of macroscopic apolar antiferroelectric (AF) to macroscopic polar ferroelectric (FE) when they are subjected to an applied electric field (Figure 4).[6,7] In addition to polarity, we must also take into account the tilt of SmC-type organization giving an added synclinic or anticlinic relation between layers as previously discussed. As shown in Figure 5, the molecules collectively turn conically when a tilted "banana" switches to align with an applied field, thereby switching both tilt and polarity simultaneously. Therefore, there is no net change in handedness and so there is both a racemic pair and an enantiomeric pair (Fig 5).

Figure 5. Racemic and enantiomeric pairs of bent-core mesogens. Reproduced from ref. 3 with permission from The Royal Society of Chemistry.

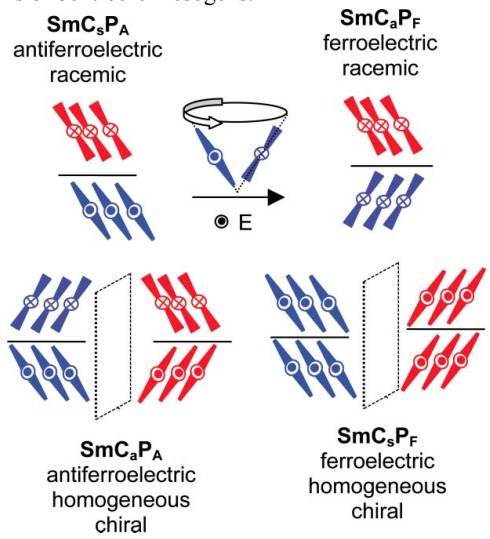

The most stable combination is synclinic AF, which is designated as SmC_sP_A. It is interesting to note that the tilted nature of the bent mesogen creates an unexpected switching pattern in that it undergoes a fast and collective rotation in a conic fashion.[3] This leads the AF

synclinic mesogen (SmC_sP_A) to switch to FE anticlinic (SmC_aP_F) upon application of an external electric field, as seen in Figure 5. It should also be noted that switching from SmC_sP_A to the SmC_aP_F state is destabilizing in terms of both polarity as discussed above, as well as its tilt where interlayer fluctuations are more hindered.[3] Even so, the energy barrier between AF and FE is small enough that we therefore observe four distinct structures based on combinations of tilt and polar directions: AF synclinic (SmC_sP_A) and anticlinic (SmC_aP_A); FE synclinic (SmC_sP_F) and anticlinic (SmC_aP_F).[4] Another interesting and important point to be noted is that having both a polar direction and a tilted direction give a handedness to the superstructure of a bent-core mesogen (Figure 6).

Figure 6. For banana mesophases, shape anisotropy combined with tilt give handedness. Reproduced from ref. 3 with permission from The Royal Society of Chemistry.

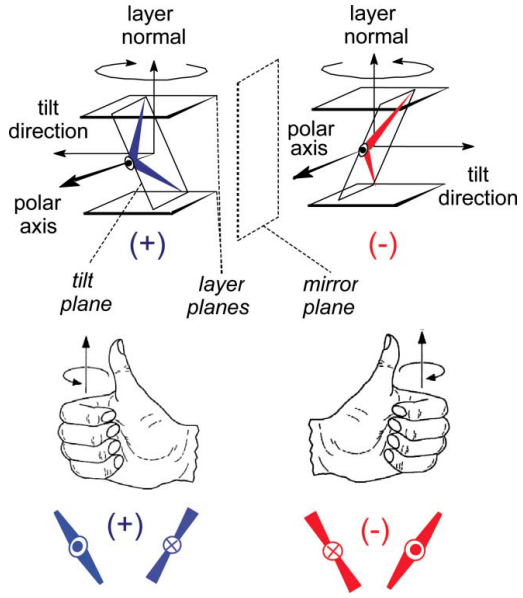

This means that bent-core liquid crystals have a chiral superstructure even if the molecules themselves are achiral. If we look at a mesogenic phase such as SmC_sP_A (Figure 5), we notice that the two layers have opposite chirality in relation to one another; one has a right-

handedness and the other a left-handedness. When both directors are switched, as in going from SmC_sP_A to SmC_aP_F, then there is no net change in handedness so the mesophase retains its original superstructural chirality. In other words, they are supermolecular racemates. However, looking at the relation between two layers such as in SmC_aP_A, we see that in fact both layers exhibit the same chirality, and so upon switching maintain the same handedness. These are therefore considered enantiomeric pairs on the superstructural level.

The chemical structure of the bent-core mesogens is what determines the ability to become a liquid crystal with its special characteristics. The central bent unit is linked to two rod-like "arms" that allow for flexibility and therefore prevent crystallization. The arms consist of aromatic rings and linking groups. Linking groups commonly include ester groups, Schiff's base, azo groups, double bonds, triple bonds, and CH_2O ether groups.[3] Ester groups and double bonds are preferred to a Schiff base as the latter is hydrolytically sensitive. The direction of the ester bond also has an important effect. For some molecules (Figure 7), when the ester bond is pointed "towards" the bent core unit, the mesophase is stabilized since the polar direction is supported. However, when they point "away," mesogenic properties are often lost and in a few cases change the type of mesophase. There are also combinations of "towards" and "away" that produce different mesophases. These affects are attenuated, opposite, or inconsequential depending on the molecule. The arms also typically end with alkoxy chains from 9 to 20 carbons that provide greater flexibility and promote FE switching of smectic phases.[4] The core length and bent angle are the most important features in the formation of the polar order. In order to maintain bent-core polar order characteristics, a bending angle between 105-140° must be maintained.[8] Outside of this range, non-polar mesophases are exhibited.[4]

Figure 7. A generalized structure of a bent core mesogen.

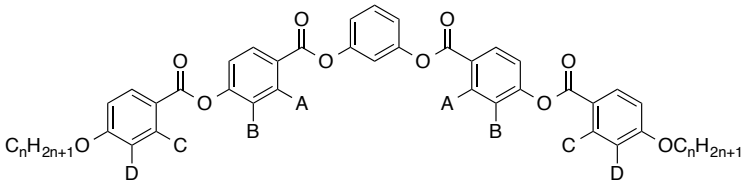

Lateral substituents have a significant influence on the self-assembled organization of liquid crystals. Fluorine, for example, is routinely incorporated as a lateral substituent in many liquid crystals. Fluorine's slightly greater size than hydrogen (1.47 Å vs. 1.2 Å) affects steric interactions without entirely disrupting Van der Waals forces, thus permitting the possibility of forming a mesophase without steric obstruction.[4] Also, as the most electronegative element, it greatly affects dipole moments, the polarization of whole π systems and the electron density of aromatic rings, thus affecting π-π stacking and π-H-C electrostatic interactions.[9-11] These effects of fluorine, however, can be stabilizing or destabilizing of the mesophase depending on its location.[12] Like the directionality of the ester group, the effects tend to be molecule dependent, but generally fluorine substituted at the central bent unit has little to no effect on the mesophase other than decreasing melting point.[13] However, fluorine substitution at certain positions on the arms can stabilize the mesophase and even change its type.[14] For an example, it was found that for the compound in Figure 7, when fluorine is substituted at position A, C or both, there is negligible effect on the mesophase. When fluorine is installed at position B alone or in any combination with B, all mesophase is suppressed. However, when fluorine is in position D, which is *ortho* to the alkoxy group, then various mesophases are generated, even for compounds that did not previously exhibit liquid crystalline phases.[12,15] In addition to fluorine, it is known that other lateral substituents, both polar and non-polar, may be inserted in various positions on the phenyl rings to induce new phases and phase sequences.[16] Other lateral substituents include

chlorine, cyano groups, and branching alkanes.[17] These substituents are important for other liquid crystalline properties, such as polymorphism. It has been demonstrated that a perfluorinated alkoxy chain at the end of an arm introduces the transformation of the non-polar, non-tilted SmA organization to SmC_a upon cooling.[18] Installing a cyano group at a position on the central angular component that is *ortho* and *para* to one of the arms leads to tri and tetramorphism.[16] This would typically follow the sequence of nematic-SmA-SmC-SmC_a. The transition from non-polar SmA or SmC to polar SmC_a is related to a continuous decrease in bending angle that can be influenced by installing large substituents such as chlorine at both *para* positions on the central core ring.[19] These are key considerations to take into account when designing and analyzing bent-core mesogens.

Radical-containing Liquid Crystals

Liquid crystals exhibit the capacity to be a functional material given their molecular anisotropy and typical π-conjugation that give rise to unique electronic properties. However, in order to construct new types of multifunctional materials, unpaired spins have been incorporated into mesogenic scaffolds. The unpaired spin allows for the possible combination of magnetic behavior and conductivity yielding the permutation of electrical properties of conventional liquid crystals with the magnetic and electronic properties of a paramagnet.[20-22] Historically, spin in paramagnetic liquid crystals comes from one of two sources; whether through coordination with a transitional metal where the permanent spin originates from either the *d*- or *f*-block orbitals, or from a stable radical of entirely organic origin.[21] For example, in 1976, the first successful report that incorporated a radical into a mesogenic scaffold in order to study the dynamic and static structure of a liquid crystalline phase through EPR.[23] In 2006, 2,2,6,6-tetramethylpiperidine-1-

oxyl (TEMPO) in a calamitic liquid crystal was synthesized in order to investigate organic-based magnetism; however the stability of the mesophase was questionable.[24] However, in 2008 Tamura incorporated a nitroxide unit as a central rigid core in a calamitic design that exhibited temperature–independent paramagnetic order in a SmC mesophase.[25] One major difficulty in using organic sources of unpaired spins resides in the typical bulkiness of radical-stabilizing substituents as well as geometrical constraints that interfere with the linearity or planarity required for mesogenic behavior.[21] Therefore, as will be further discussed in the section on the project outline, the verdazyl radical was our choice given its robustness, planarity and ideal substitution positions to produce bent-core mesogens.

The Verdazyl Radical

Our research group pioneered the use of the verdazyl radical as a structural element of liquid crystals. The verdazyl, first discovered by Kuhn and Trischmann in 1963,[26] is a stable radical and therefore isolable, and neither does it dimerize in the solid state nor in solution. (Figure 8).[27]

Figure 8. a) Kuhn's verdazyl, b) 6-oxoverdazyl, and c) DDPH, a hydrazyl radical.

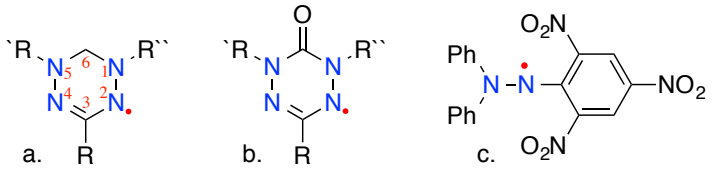

The verdazyl is a unique compound, even among stable radicals. It is similar to other hydrazyl radicals, such as *N*,*N*-diphenyl-*N*-picrylhydrazyl (DDPH) shown in Figure 8c,[28] in that the unpaired electron constitutes the singly occupied molecular orbital (SOMO) which is the

anti-bonding π^* orbital and spans all four nitrogens (Figure 9a).[29] Several methods of spectroscopic analysis have been applied to the verdazyl to study its electronic structure that include EPR, ENDOR, and NMR as well as computational investigation using DFT methods.[30-34] Through these methods, it has been demonstrated that the unpaired electron is a part of a 7π electron system delocalized over the N1-N2-C3-N4-N5 atoms, resulting in two pairs each of zwitterionic and diazaallyl-type nitrogens as depicted in Figure 9b.[34] The unique stability[28,35] of the radical is mainly due to the delocalization of the radical and the fact that the SOMO is the anti-bonding π^* orbital,[36,37] and therefore the verdazyl exhibits diverse characteristics and reactivity.

Figure 9. a) 7π electron resonance of the verdazyl, adapted from Hicks.[34] b) The SOMO of the verdazyl (left) and spin density (right) are shown. Reproduced from ref. 37 with permission from The Royal Society of Chemistry.

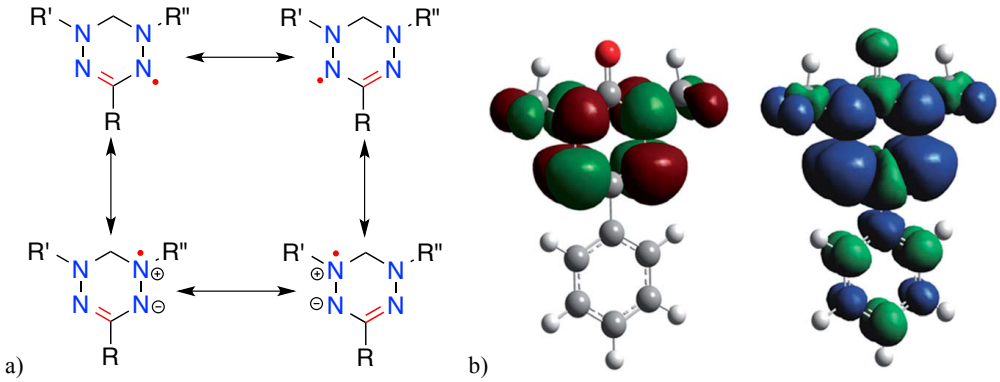

The C6 carbon is excluded from spin delocalization because it is either a saturated sp^3 carbon (Kuhn's radical) or part of an exocyclic double bond (i.e. 6-oxoverdazyl).[32] Kuhn's verdazyl (Figure 8a) having a saturated C3, takes on a half boat configuration whereas the sp^2 carbon in the 6-oxoverdazyl allows for the ring to be nearly planar.[35,36,38] An aryl group substituted on the C3 position is nearly coplanar with the ring while aryl group on the N1 and N5 positions are twisted at ~30° with respect to the ring (Figure 10).[36,38]

Figure 10. Crystal structures from Neugebauer of a) 6-oxoverdazyl and b) Kuhn's verdazyl. Reproduced from ref. 36 with permission from The Royal Society of Chemistry.

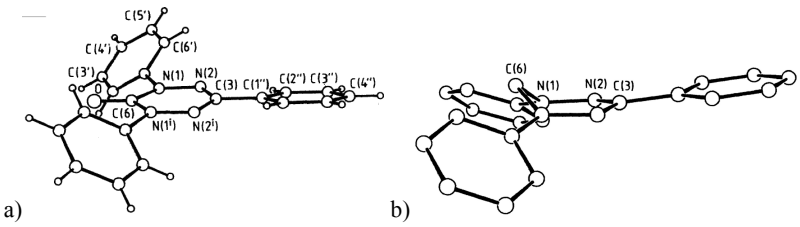

As we can see in Figure 10, the delocalization of the unpaired electron is retained within the ring and does not transfer to substituents on C3 since a nodal plane of the SOMO passes through both C3 and C6. This node prevents the π framework of the C3 substituent from conjugative overlap with the SOMO. [34,37] Among the two types of nitrogens, more spin density is observed on the N2 and N4 nitrogens in the 6-oxoverdazyl resulting from the electron withdrawing effects of the carbonyl and polar resonance structure.[34] There is, however, a negligible amount of spin on the C3, C6 and C6 substituents through spin polarization.[34]

The verdazyl's redox capacity in electron transfer reactions has been explored demonstrating that the radical can undergo one-electron redox reactions as seen in Scheme 1.[34] Substituents on the nitrogens influence the electronic structure and properties of the verdazyl since they are attached to the ring with access to the SOMO.

Scheme 1. One electron redox reactions of the verdazyl.

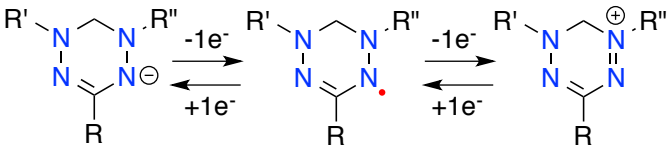

Under certain conditions, the unpaired electron can undergo chemical reactions. During hydrogenation, the radical is reduced and yields the *leuco* form of the verdazyl which is no

longer paramagnetic and is colorless (Scheme 2).[40] The N-H bond of the *leuco* is relatively weak at ~70 kcal/mol as compared to 93 kcal/mol for a standard amine.[41]

Scheme 2. Hydrogenation of the verdazyl produces tow possible tautomers of the un-isolable *leuco* form.

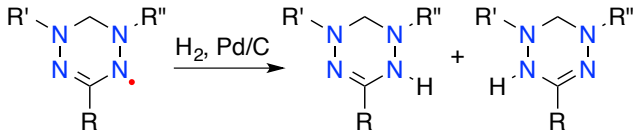

The verdazyl heterocycle is also capable of undergoing reactions with organometallic reagents as diagrammed in Scheme 3.[34,42] Here, the verdazyl is initially reduced by the carbanion resulting in a carbon radical, and the verdazyl is subsequently either metallated or alkylated at the N2/N4 nitrogen.[34,39]

Scheme 3. Verdazyl reactions with organometallic reagents.[Adapted from ref. 34.]

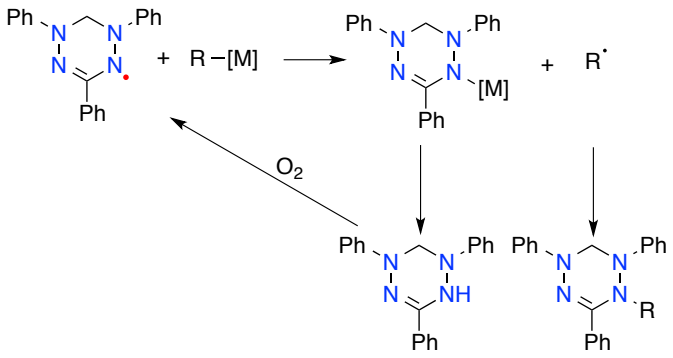

Verdazyl-based Liquid Crystals

Although there have been fundamental research on the conductivity and magnetism of the verdazyl, these were performed using the verdazyl in the solid state and with limited variety of substituents.[43] The area of greatest difficulty in using organic material that exhibits both conductive and/or magnetic capabilities is the design of molecules that will allow for correct

alignment into a semiconducting channel and with correct alignment of spins.[43-46] The manner in which the molecules pack into a crystalline structure dictates if the material will be a semiconductor or exhibit magnetic behavior, and if it does, the type of electronic properties or magnetism displayed.[47] Therefore, it is essential to carefully design a molecule that will self-assemble into a 3D material as desired. As can be expected, however, this is only accomplished through a tedious trial and error process of design, synthesis, and analysis of the physical structure of the bulk material and electronics of the individual molecules.[48]

Addressing and overcoming these challenges, our group has been working on the incorporation of a stable radical into a liquid crystalline structure. Several years ago, the group focused on the verdazyl and began to publish work in regard to the incorporation of the verdazyl as the central rigid core unit in the design of discotic mesogens with both alkoxyl[49] and alkylsulfanyl[49,50] substituents (Figure 11) that exhibited liquid crystalline columnar mesophases, thus generating alignment of the verdazyl units that would be appropriate for photoconduction. Therefore, both magnetic and electronic character were studied in addition to exploring mesogenic behavior. Charge photogeneration and its transport in a liquid crystalline radical were demonstrated for the first time.[50] These discotics also exhibited paramagnetic behavior close to that of an ideal paramagnet.[49]

Figure 11. Verdazyl-containing discotic mesogens.[49]

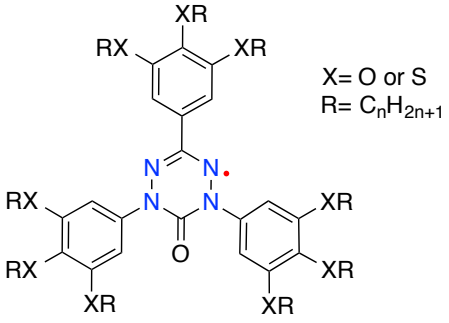

In the fall of 2014, the group published work that utilized the verdazyl as the central rigid core unit of bent-core molecules.[51] A series of symmetrical, banana-shaped derivatives of a verdazyl with a trifluoro group at the C3 position (Figure 12). An important discovery that came from this study was not only interesting mesophases, but in fact a new phase was demonstrated. The materials exhibited paramagnetic behavior and photogenerated ambipolar charge transport.

Figure 12. Verdazyl-containing bent-core mesogens of the CF_3 derivatives.[51]

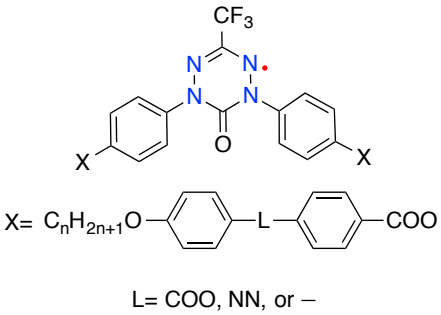

Project Outline

In light of these discoveries and insights, my project is to study paramagnetic bent-core mesogens using the verdazyl radical as the central rigid core unit. The design of these mesogens includes constructing dissymmetric mesogens since we anticipate lower melting temperatures, and therefore liquid crystalline behavior that is more attractive for application. Given their molecular shape, bent-core molecules are susceptible to external stimuli, and thereby allow us to manipulate their physical arrangement in the mesophase.

We proposed that the verdazyl radical could be the key element of organic-based paramagnetic bent-core semiconductors given that it possesses a combination of desirable properties. The verdazyl is ideal since it has an open-shell π electron for facile generation of charge transport,[50] planarity of the heterocyclic ring that is ideal for molecular stacking in the

mesophase, potential substitution pattern allowing for proper bent-core geometry, as well as its overall robustness. In order to accomplish our goal, we use fundamental knowledge of bent-core mesogens as our guide to construct molecules that may exhibit banana mesophases. Thus, by designing molecules with the verdazyl radical as a central core unit and installing substituents that will induce mesogenic behavior, we are constructing paramagnetic liquid crystals to take advantage of their inherent self-assembled organization for the alignment of the verdazyl units to ensure that the molecular stacking has sufficiently close face-to-face π-π contact between each stacked layer of molecules and therefore attain a conducting channel.[16,52-54] As we generate mesophases and gain a greater understanding of structure-property relationships, we can incorporate essential structural changes at the molecular level to allow for greater packing density, which translates into more efficient charge transport.[52]

Although the verdazyl radical has been investigated for four decades, extensive functional group transformation on the N1- and N5-substituents has been lacking. This is not surprising given the fact that these substituents are in conjugation with SOMO of the verdazyl, which may be expected to interfere with these transformations. Therefore, we needed to first establish the scope of functional group manipulation on the substituents of the verdazyl. In this way, we mean to demonstrate the range of functional groups and experimental conditions that are compatible with this radical. With effective synthetic methodologies in hand, we then prepared appropriately substituted verdazyl derivatives and demonstrated that bent-core verdazyls have the potential to exhibit banana mesophases.

In summary, we discovered reaction conditions for functional group transformation on verdazyl substituents, designed bent-core molecules based on our discoveries, and then studied what substituents are necessary for the verdazyl-based molecules to display mesogenic

properties. Once structure-property relationships are fully established, we will then investigate the functional character of the material. One challenge to this project is detection and characterization of the verdazyl radicals. Nuclear magnetic resonance (NMR) is applied limitedly since once the tetrazine is oxidized to the verdazyl radical, detection of signals and determination of the chemical structure of the paramagnetic material is futile due to broadened signals and diminished resolution and therefore inability to resolve coupling. Detection is then accomplished by high-resolution mass spectrometry (HRMS) for all verdazyls. Characterization is given by elemental analysis, melting point, FTIR and UV-*vis*. Thermal analysis by differential scanning calorimetry (DSC) revealed exothermic and endothermic transitions during melting and cooling that correlate to phase transitions between the crystal state, mesophase, and isotropic liquid. The use of polarizing optical microscopy provided phase identification.

Chapter 2: Experimental results

Studies on Functional Group Transformation:

To explore the scope of functional group transformation (FGT) on the *N*-substituents of the verdazyl, we began with synthesizing the 6-oxoverdazyl with varying functional groups on phenyl substituents on the N1 and N5 nitrogens. Using the Milcent method to synthesize the tetrazine precursor to the verdazyl (Scheme 4) allows us to easily obtain various phenyl-substituted functional groups (FG).[56]

Scheme 4. Generalized and modified Milcent method for preparation the tetrazine heterocycle.

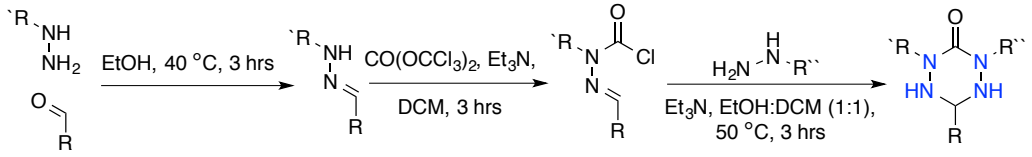

Thus, we began with the condensation of 4-nitrophenylhydrazine and benzaldehyde to produce the hydrazone **1a**[57] in a high yield typically around 95%, which was then reacted with triphosgene to give the carbamoyl chloride **2a**[56] again in high yield around 93%. Reacting chloride **2a** with a series of 4-substituted phenylhydrazine of choice resulted in the formation of tetrazines **3** (Scheme 5).[58]

Scheme 5. Milcent's method for preparation of tetrazine **3**.

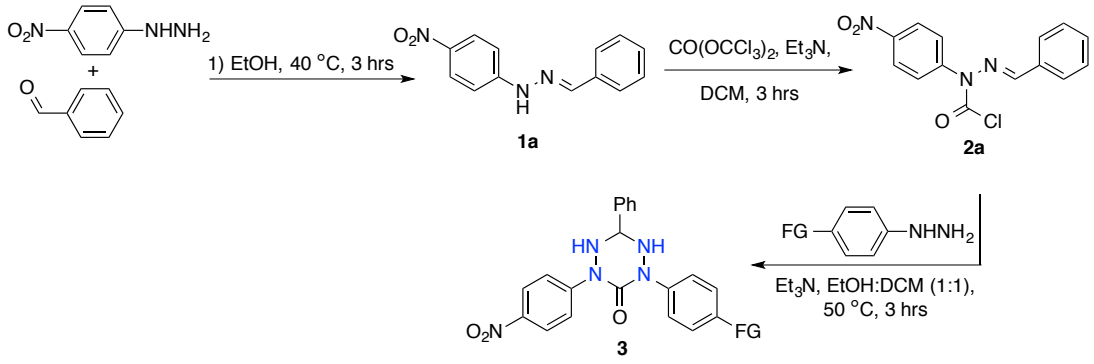

The hydrazines may be custom made in the lab or bought commercially. Tetrazines **3** were synthesized in yields ranging from 30-72% from the carbamoyl chloride **2a**. The variation in yields is rationalized by the effectiveness of the substituent on the phenylhydrazine to be able to increase the nucleophilicity of the *β*-nitrogen, thus affecting the regioselectivity of acylation and ring closure. The tetrazine is subsequently oxidized by a mild oxidant such as $NaIO_4$, $K_3Fe(CN)_6$, or PbO_2, to the verdazyl (Scheme 6).

Scheme 6. Preparation of the verdazyl by oxidation of tetrazine using either $NaIO_4$, $K_3Fe(CN)_6$, or PbO_2.

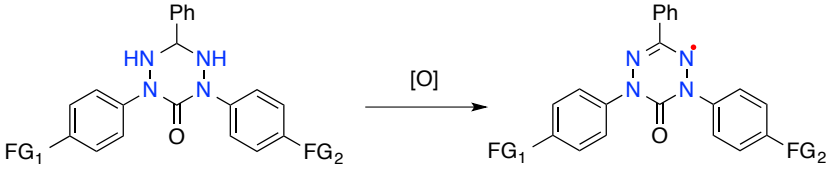

Upon successful oxidation to the verdazyl, FGT is pursued and the scope of investigation is summarized in Scheme 7.

Scheme 7. Functional group transformation explored on 6-oxoverdazyl.[58]

1) $-NO_2 \Rightarrow -NH_2 \Rightarrow -NHCOR$

2) $\begin{matrix}-OBn \\ \text{or} \\ -OCOPh\end{matrix} \Rightarrow -OH \Rightarrow \begin{matrix}-OR \\ \\ -OCOR\end{matrix}$

3) $-COOH \Rightarrow -COOR$

4) $-I \Rightarrow -Ar$

C3-phenyl Verdazyls:

Functional Group Transformation of $-NO_2 \Rightarrow -NH_2 \Rightarrow -NHCOR$ and $-OBn \Rightarrow -OH \Rightarrow -OR$:

Reacting benzaldehyde α-chloroformyl-4-nitrophenylhydrazone[56] with 4-benzyloxy-phenylhydrazine[57] to form the tetrazine **3a** proceeded in 72% yield. In general, the tetrazine heterocycle was found to be somewhat sensitive to the mild acidity of silica gel used for chromatography, regardless of substituents. Therefore, a small portion of Et_3N was used during the preparation of the column to pacify the gel. Purified tetrazine **3a** was then subjected to oxidation to verdazyl **4a** with $K_3Fe(CN)_6$ in 86% yield, as shown in Scheme 8, which allowed us to begin FGT studies.[58]

Scheme 8. Formation of the verdazyl **4a** using Milcent's method.

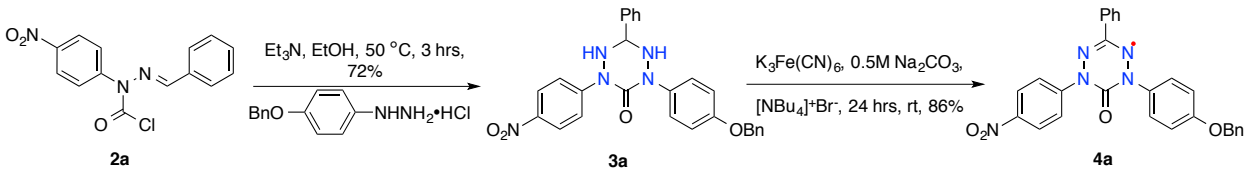

The first action we took was to attempt reduction of the nitro group in **4a** to the amine, which was easily accomplished by hydrogenation with H_2 at 50 psi and a catalytic amount of PtO_2 in a yield of 82% (Scheme 10). The concomitant reduction of the verdazyl to the *leuco*

form **5a** was evident as the solution became colorless. Therefore, **5a** was aerially re-oxidized by bubbling air through the solution for approximately 1 hr after which it was noted that the solution had returned to a deep purple color, thus indicating the presence of the verdazyl radical **6a** (Scheme 9).

Scheme 9. Aerial oxidation of the *leuco* form to the verdazyl.

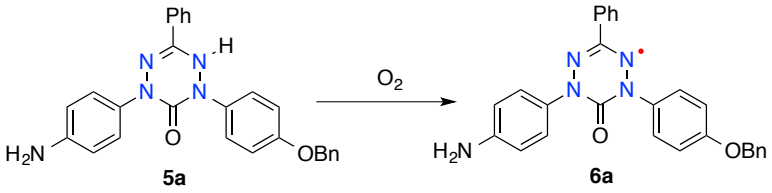

The subsequent amidation of **6a** with benzoyl chloride and organic base proceeded unremarkably giving the desired amide, **4b**, in 67% yield (Scheme 10). Turning our attention toward the other FG, debenzylation of **4b** using H_2 and Pd/C at atmospheric pressure and ambient temperature was attempted. The reaction did not afford the desired deprotection of the phenol but instead, after aerial workup, gave only starting material **4b** after 24 hours.[58] The reaction was periodically monitored and allowed to proceed for 168 hours, after which analysis demonstrated only starting material and decomposition products. Increasing the pressure to 50 psi proved successful as the reaction was complete in 2 days giving a 58% yield of the phenolic intermediate after aerial oxidation. The phenol (not shown) was then esterified with benzoyl chloride in the presence of Et_3N yielding ester **4c** in 74% yield (Scheme 10). Starting from condensing benzaldehyde and 4-nitrophenylhydrazine, the synthesis of **4c** was completed in 8 steps and 13% overall yield.

Scheme 10. Functional group transformation of $-NO_2$ and $-OBn$.

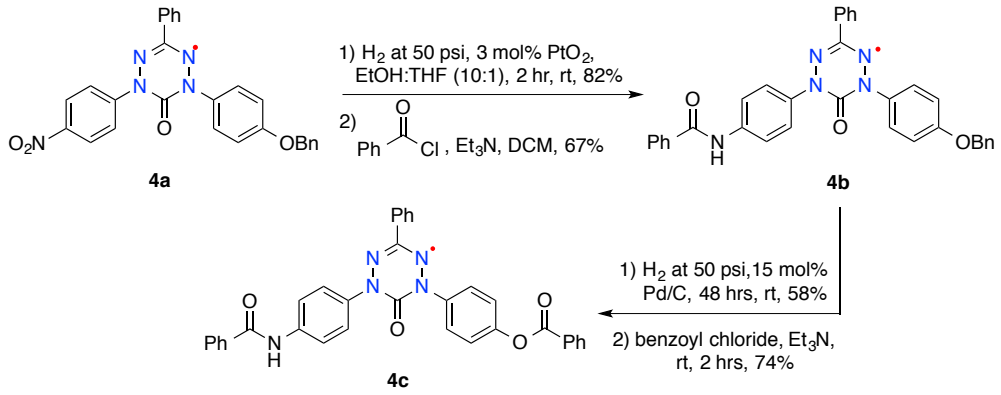

Functional Group Transformation of $-COOH \Rightarrow -COOR$:

Similarly, chloride **2a** was reacted with 4-carboxyphenylhydrazine under typical Milcent conditions, with the exception of an additional equivalent of Et_3N, giving a low but anticipated yield of **3d** at 30% (Scheme 12). The carboxyl tetrazine derivative **3d** was then oxidized with either $K_3Fe(CN)_6$ or $NaIO_4$ in the presence of aqueous Na_2CO_3 (Scheme 11). Transformation to verdazyl **4d** was apparent as the reaction mixture attained a dark red color; however as the reaction was left to continue to completion, all radical was lost giving a brown reaction mixture. Attempted isolation of the radical after 2 hours resulted in an unstable dark red compound presumed to be radical **4d** that lost its color within minutes (Scheme 11).[58]

Scheme 11. Unsuccessful attempt to isolate **4d**.

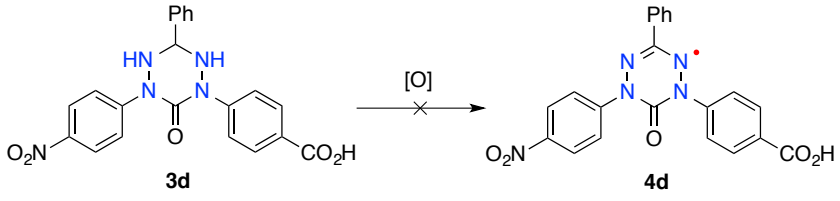

For synthetic utility, it was decided to esterify the acid at the stage of the tetrazine **3d**, which proceeded in 60% yield through a DDC coupling, which was then oxidized to the verdazyl **4e** with $K_3Fe(CN)_6$ in 97% yield (Scheme 12).[58]

Scheme 12. Synthesis of **4e**.

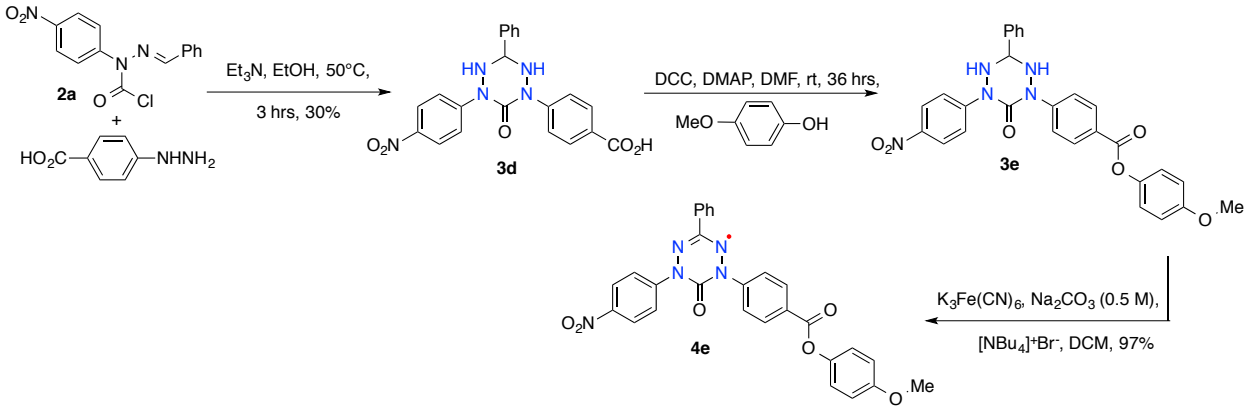

Functional Group Transformation of −I ⇒ −Ar:

Following the procedure for the preparation of tetrazine **3a**, chloride **2a** was cyclized with 4-iodophenylhydrazine to give the iodo-tetrazine **3f** in a yield of 90%. Subsequent oxidation of **3f** gave the verdazyl **4f** in a yield of 70% (Scheme 13). With the iodo-substituted verdazyl **4f** in hand, a Negishi-type cross-coupling reaction[59,60] was pursued. The Negishi reaction was initially chosen for cross-coupling on **4f** since it provides mild conditions that we anticipated would be more compatible in the presence of the radical. However, the Negishi reaction with **4f** was found to produce only presumed decomposition, and no amount of either starting material **4f** or product **4g** was observed by TLC analysis, NMR, or HR-MS.

Scheme 13. Cross-coupling attempts on the iodo-verdazyl **4f**.[58]

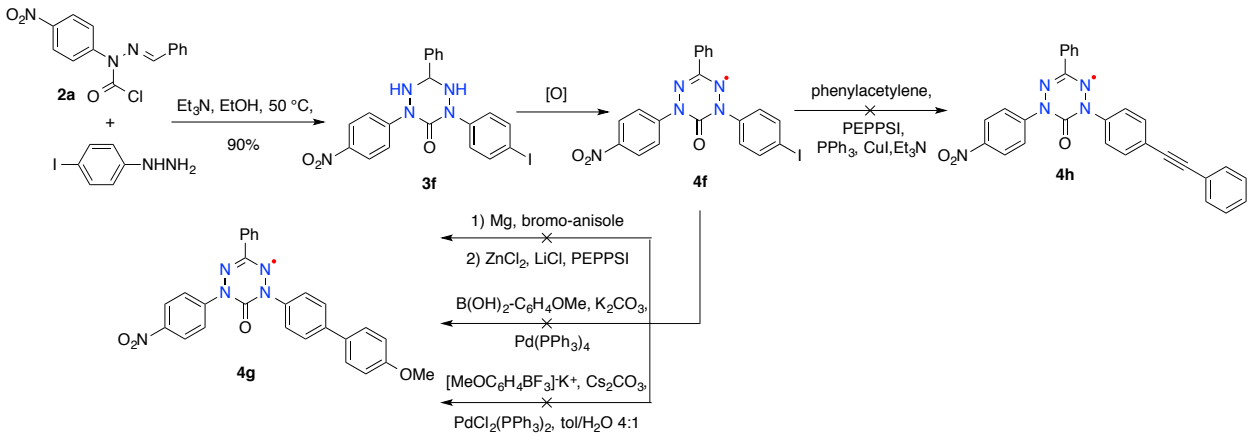

Other cross-coupling reactions were also attempted, such as Sonogashira,[61] Suzuki[62] and Molander's modification[63] of the Suzuki coupling. Unfortunately, all cross-coupling attempts resulted in a similar outcome as the Negishi reaction. In order to confirm that conditions were in fact appropriate and conducive to cross-coupling, a parallel reaction was simultaneously performed under the same reaction conditions using 4-pentylphenyl 4-iodobenzoate as the control, resulting in the coupled product. In a parallel strategy to the carboxyl derivative, all cross-coupling reactions mentioned were also performed on the tetrazine precursor **3f**, yet results showed similar decomposition-type products. There is speculation that in the presence of the Pd catalysts used, there may be oxidative addition of one of the nitrogens of the heterocycle into the Pd followed by the rupture of the relatively weak N-N bonds of the verdazyl, thus leading to decomposition, but at this point a definitive mechanism to explain the rationale for the observed decomposition has not been proven.

N1-methyl Verdazyls:

N-*methyl derivative with C3 pre-functionalized arm*:

With these synthetic methods established, we began work toward the formation of banana-phase mesogens. Desiring to introduce dissymmetry to our mesogenic scaffold, 1,3-substitution was introduced. We anticipated that this dissymmetry would allow for lower clearing and melting points. Our strategy was to construct one "arm" of the mesogen at the initial synthetic stages, then install the second "arm," and thereby providing access to our bent-core molecule, as shown in Scheme 14. Thus, capping the phenolic group of 4-hydroxybenzaldehyde with a long alkyl chain, the arm was synthesized through sequential oxidation reactions to the carboxylic acid using potassium permanganate and esterifications by conversion to the acid chloride with $SOCl_2$ to eventually obtain aldehyde **7a**[64] in 66% yield over 5 steps. Subsequent condensation of **7a** with 4-benzyloxyphenylhydrazine, and continuing the Milcent method until the formation of tetrazine **3v**.

Scheme 14. Preparation of tetrazine **3v** with a "pre-functionalized arm."

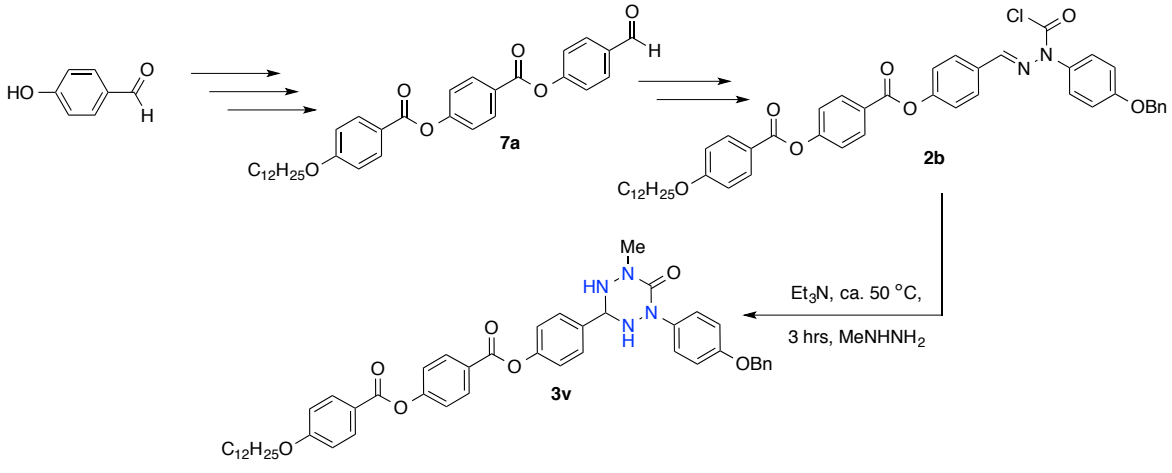

Although chemistry up until the carbamoyl chloride **2b** proceeded with ease, formation of the heterocycle proved problematic. As we can see from Table 1, the strategy of constructing a pre-functionalized arm proved less fruitful than hoped for.

Table 1. Comparison of solvent dependent yields of formation of tetrazine **3v**.

Solvent	Yield
C_6H_6	0-5%
EtOH	neg.
DCM:EtOH (1:1)	<15%
DCM	15%
THF	0%

N-*methyl, bis-benzoyloxy derivative*:

Among the various solvent systems, DCM was the only solvent to yield desirable results. In one trial, **3v** was produced at 24% but was irreproducible at that yield. The most consistent yield, however, was 15%. Therefore, given the inconsistent and low yields, it was decided to revise the synthetic strategy by simply constructing a smaller molecule that contains two protected phenolic functionalities, in parallel to our protocol that allowed us to establish the fundamental studies to understand functional group transformation methods. Thus, chloride **2d** cyclizes with methylhydrazine to form the tetrazine **3i** in a moderate yield of 66% (Scheme 15).

Scheme 15. Formation of verdazyl **4i**.

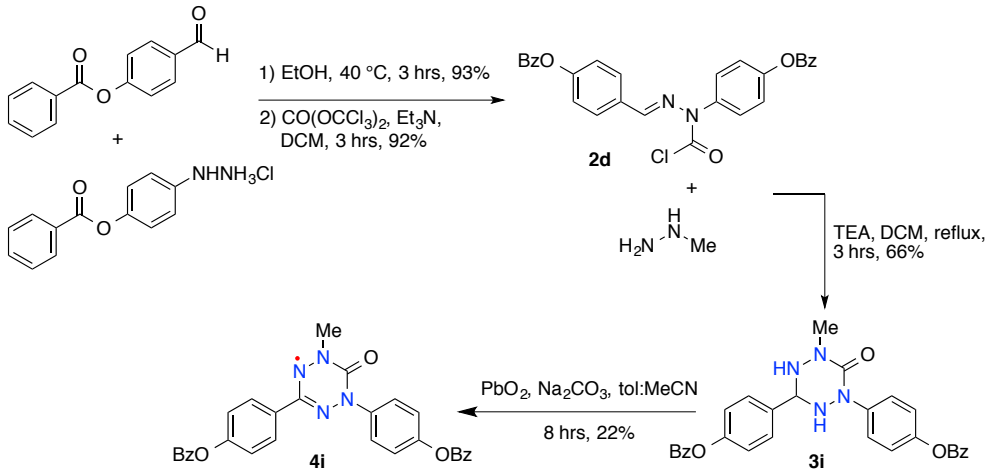

Purification of tetrazine **3i** was hindered by sensitivity to the acidic conditions of chromatography with silica gel. Subjecting this compound to a passivated silica gel column, as previously described, resulted in total loss of the product. This was largely overcome by replacement of silica with Florisil® gel followed by recrystallization giving **3i** in 66% yield. Oxidation of **3i** also proved problematic which was not particularly surprising as there was literature precedent for a lessened stability of an *N*-methyl substituted verdazyl which readily undergoes disproportionation with the open-shell electron, when compared to an *N*-aryl substituent.[65] Monitoring by TLC, formation of verdazyl was accompanied by the possible disproportionation product, thus resulting in the notable loss of verdazyl with the concomitant formation of the presumed disproportionation products. Therefore, verdazyl **4i** was isolated after 3 hrs with a yield of 22% (Scheme 15).

Noting the sensitivity of tetrazine **3i**, it was exposed to air to attempt aerial oxidation to **4i**. Noticeable coloration of the purified, white crystals of tetrazine **3i** to a light pink began after two days of aerial exposure. After 10 days, the color had become dark pink. TLC analysis showed the probable formation of desired verdazyl **4i** along with small amount of side products,

and HRMS notes a mass corresponding to a protonated verdazyl **4i**. Considering the instability of *N*-methyl verdazyl derivatives, this route will not be continued and so this represents our progress toward this verdazyl derivative at this point in time.

N1-phenyl Verdazyls:

N-*phenyl, bis-benzoyloxy derivative*:

Noting the problematic synthesis of verdazyl **4i**, it was decided to employ the phenyl group at the head position so that disproportionation would not be possible. Thus, condensing chloride **2d** with phenylhydrazine gives tetrazine **3j** in 62% yield, which is then smoothly oxidized to the verdazyl **4j** in 55% yield with PbO_2 and 81% with $K_3Fe(CN)_6$ (Scheme 16).

Scheme 16. Synthesis of verdazyl **4k**.

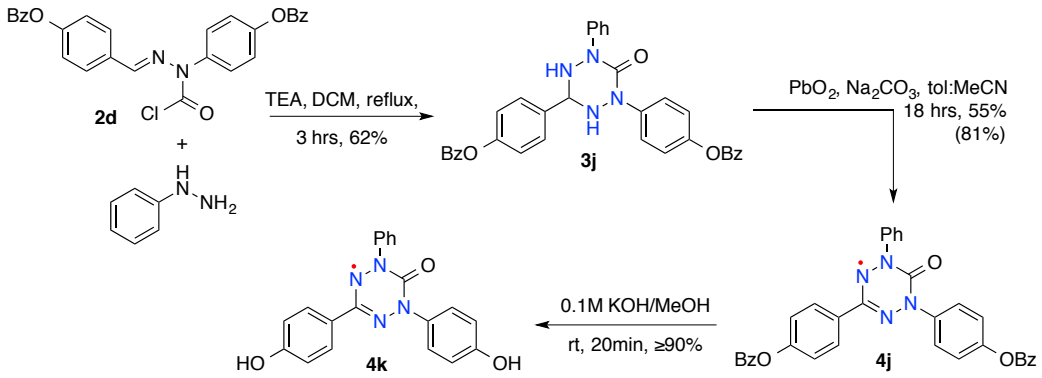

The structure of tetrazine **3j** was confirmed by a H^1-NMR *COSY* experiment which demonstrated a spin system corresponding to the N2-C3-N4 hydrogens (Figure 13).

Figure 13. *COSY* correlations between N2-C3-N4 hydrogens.

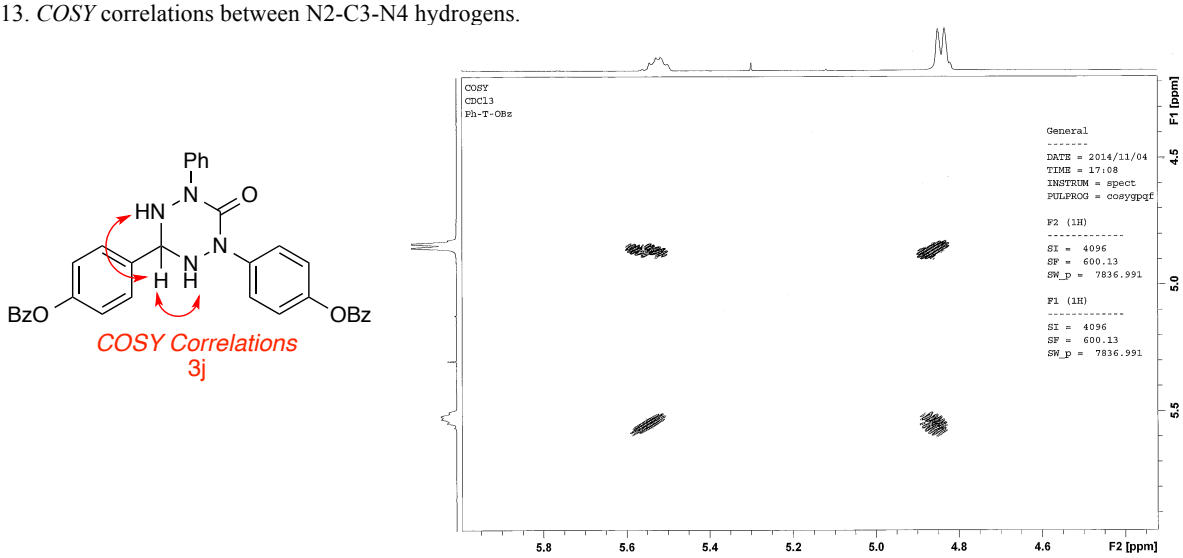

In order to further analyze radical **4j**, it was subjected to a hydrogen atmosphere using Pd/C as the catalyst to obtained the *leuco* form, **5j** was generated in under 5 min., (Scheme 17). While **5j** was not isolated, it was analyzed directly in the reaction vessel by NMR, providing a rare spectroscopic characterization of the *leuco* form. Interestingly, an H^1-NMR experiment in a field of 400 MHz showed a singlet at approximately 6.1 ppm with an integration of 1 proton, whereby analysis at 600 MHz resolved the signal into two singlets, each with an integration value of a half proton, thus revealing two tautomers of the *leuco* form **5j** in a 1:1 ratio (Scheme 17).

Scheme 17. a) Reduction of verdazyl **4j** to the *leuco* form **5j**. b) H^1-NMR of the tautomeric proton.

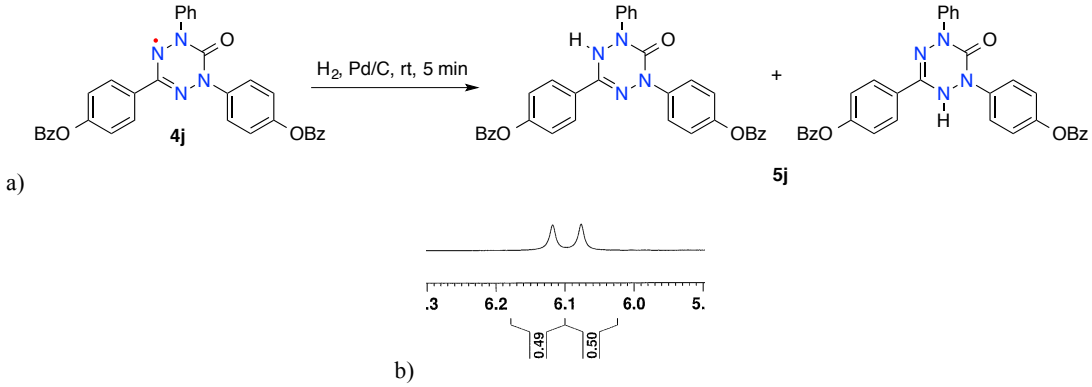

With the phenyl as the head group and two aryl-substituted benzoyloxy functional groups, we then advanced toward our goal of forming bent-core mesogens. Saponification of the ester gave the phenolic functionality in **4k** in high yield at 90% (Scheme 16). Esterification of **4k** was accomplished either through DCC coupling or by acylation with the acid chloride, the latter method generally resulted in greater yields in significantly shorter reaction times. Thus, we have obtained a small library of bent-core molecules as shown in Scheme 18.

Scheme 18. Formation of a series of bent-core molecules.

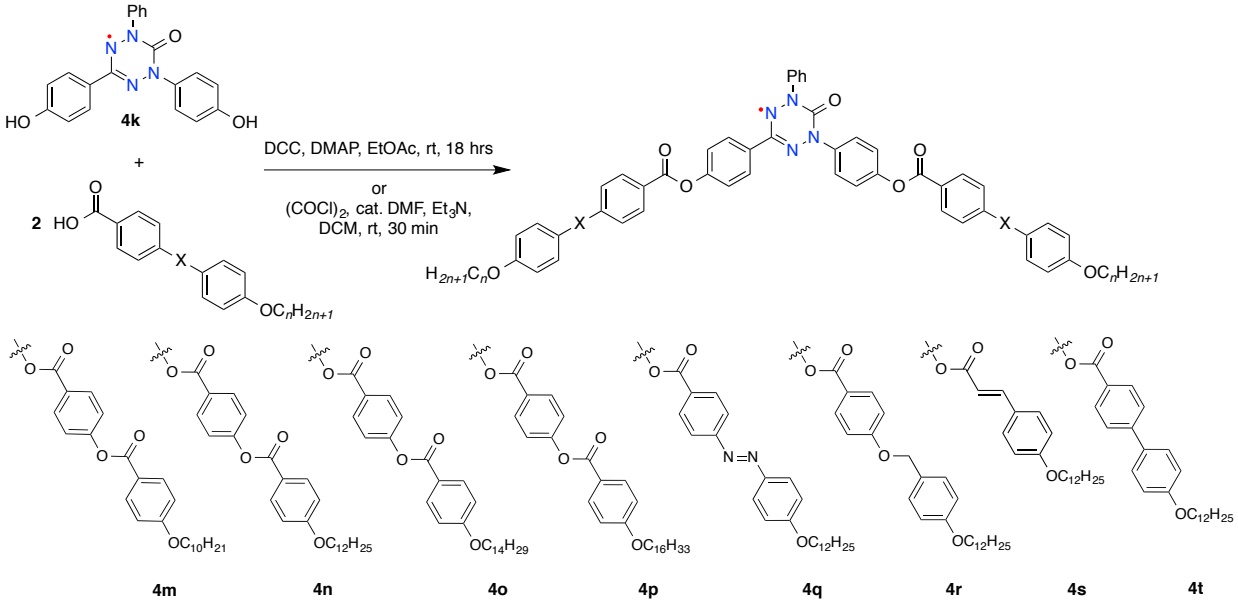

By varying linking groups and lengths of the alkoxy chains of the arms, we are able to establish relationships between molecular structure and thermal property for the series of bent-core molecules. The synthesis requires only six steps starting from condensing the aldehyde and hydrazine, and is moderately efficient (e.g., 36% for **4n**). Thermal analysis by differential scanning calorimetry (DSC) reveals exothermic and endothermic transitions during melting and cooling that correlate to phase transitions between the crystal state, mesophase, and isotropic liquid. The use of polarizing optical microscopy provided phase identification.

As seen in Scheme 18, eight verdazyls that were functionalized in a bent-core fashion have been synthesized, three of which demonstrated mesogenic behavior as summarized in Table 2. Two series of compounds were prepared. In the first series (**4m**-**4p**), the length of the alkoxy chain was varied from 10 to 16 carbons while maintaining the ester linking group. We then compared linking group variations while maintaining the length of the alkoxy chain at 12 carbon atoms (**4n**, **4q**-**4t**). Analysis by DSC and POM reveals that BCMs with arms that contain a carboxyl linking group and alkoxy chains from 10-14 carbons exhibit SmA mesophase behavior. All other combinations did not result in any mesophase, including the derivative from cinnamic acid, **4s**. The results are summarized below in Table 2.

Table 2. Summary of bent-core mesogens synthesized.

Compound	L	n	Mesogenic behavior	% Yield
4m	-COO-	10	Cr 127 (SmA 114) I	72
4n	-COO-	12	Cr 118 (SmA 104) I	65
4o	-COO-	14	Cr 117 (SmA 118) I	74
4p	-COO-	16	Cr 110 I	69
4q	-N=N-	12	Cr 94 I	65
4r	$-CH_2O-$	12	Cr 96 I	51
4s	*	12	Cr 84 I	70
4t	–	12	Cr 134 I	68

Studies are shown in scheme 18.
* = **4s** is a cinnamic ester derivative.

We see from Table 2 that increasing the length of the carbon chain while maintaining the ester linking group leads to a decrease in the melting point of the material. Since the carbon chains provide for mobility of the molecules, and therefore the ability to flow and potentially self-assemble, we can rationalize that longer chains will provide greater mobility, and thereby lower the melting point. We note that only the shorter chain lengths with ester linking groups exhibit mesogenic behavior, all of which exhibit monotropically during the cooling of the material. By this, we may understand that a chain length of 16 carbons is apparently outside of the range of acceptable overlap of molecules for efficient layer modification during self-assembly, thus leading to the disruption of the mesophase behavior. While we can clearly discern a trend in the melting points in the first series, we do not, however, see a predictive tend in the clearing temperatures of the mesophases of the materials. When considering the second series where the chain length is maintained while varying the linking groups, we see that the azo, ether, and cinnamic acid derivatives melted below their ester and bi-phenyl counterparts.

N1-thiophenyl Verdazyl:

Given that the *N*-substituted phenyl group possesses an approximately 30° twist to the planar heterocycle, then altering the head group will almost certainly change the packing density and layer organization of the liquid crystal. To investigate this, a thiophene unit was installed as the head group by first synthesizing 2-thiophenylhydrazine **9a**. Lithiated thiophene performs a nucleophilic addition to di-*tert*-butyl azodicarboxylate (DTBAD) yielding the hydrazide **8a** in a 93% yield over a two-step process (Scheme 19).

Scheme 19. Formation of the electron rich thiophenyl hydrazide **8a**.

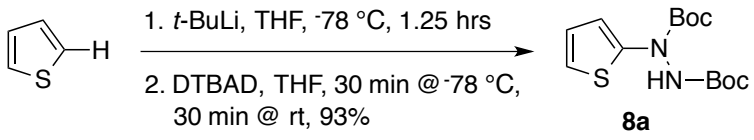

In a previous study performed by our group,[66] *tert*-butyloxycarbonyl (Boc) protected electron-rich hydrazines were shown to be most efficiently deprotected using trifluoromethanesulfonic acid (TfOH) in 2,2,2-trifluoroethanol. The Boc groups were then removed using slight modifications of the reported procedure. The reaction was initially run at -40 °C which resulted mostly in starting material and some formation of the desired product, but upon raising the temperature to 0 °C, product consistently formed in 89% yield as a viscous yellow oil, with both NMR and TLC analysis showing high purity of a single compound (Scheme 20).

Scheme 20. Formation of the thiophenyl substituted tetrazine.

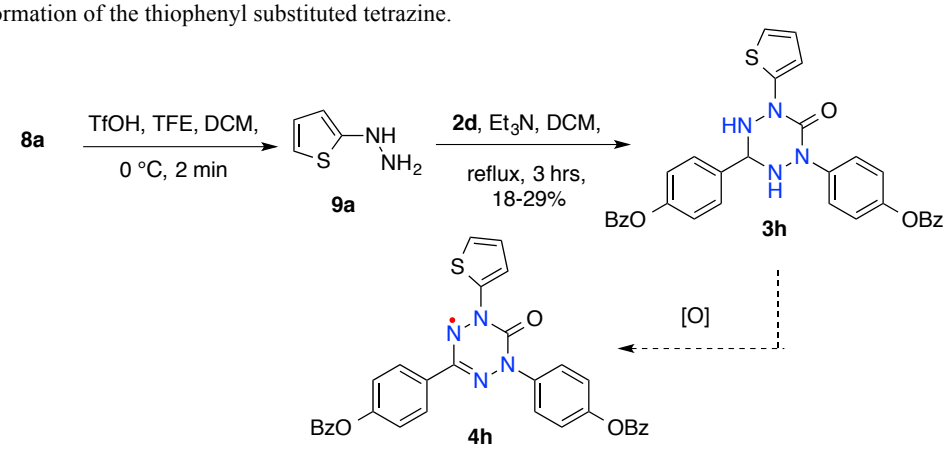

As expected with electron-rich hydrazines, gradual decomposition ensued upon deprotection owing to oxidative instability that was indicated by severe darkening of the

substance until complete decomposition around 30-40 minutes later, which was confirmed by H^1-NMR. In order to avoid complications from thermal decomposition during cyclization, carbamoyl chloride **2d** was immediately reacted with crude hydrazine **9a** to produce the tetrazine **3h**. This reaction was inconsistent, giving yields ranging from 18-29% after SiO_2 purification over multiple trials, likely due to the instability of the hydrazine. Different solvents were tested resulting in DCM:EtOH (1:1) producing the desired product with benzene and THF yielding no reaction. Oxidation of **3h** to the verdazyl (not shown) was also problematic. Both $NaIO_4$ and PbO_2 had no effect on the tetrazine while $K_3Fe(CN)_6$ had presumably procured the verdazyl in a meager 24% over 9 hours with some unreacted starting material still present. However, when the reaction was left over night, all product and starting material were lost.

Chapter 3: Discussion and Conclusions

We discovered that under appropriate conditions, functionalization of the N1/N5 aryl-substituents is possible allowing for synthesis of mesogenic "arms." Consequently, functional group transformations allow us to build molecular structures typical of bent-core mesogens. The thermal properties of these compounds were characterized by DSC, and phase identification by (POM) optical microscopy. These analyses revealed that bent-core molecules that incorporate the verdazyl as the central rigid core unit, are capable of exhibiting mesogenic behavior. Derivatization of the arms containing varying linking groups allows for broader structure-property relationship studies, and are ongoing at this time. Varying the head group from phenyl to either methyl or thiophenyl should also introduce variation in mesophases and therefore stacking orientation.

Chapter 4: Procedures

4-(4-(4-(Dodecyloxy)benzoyloxy)benzoyloxy)benzaldehyde 4-benzyloxyphenylhydrazone (**1b**):

An Ar-flushed round bottom flask was charged with aldehyde **7a** (2.00 g, 3.77 mmol) in EtOH (25 mL) and 4-benzyloxyphenylhydrazine chloride (1.89 g, 7.54 mmol) and stirred at 40 °C for 3 hrs. The reaction was then evaporated followed by recrystallization from EtOH to obtain 2.55 g (93% yield) of pure hydrazone as light pink crystals: mp 177.2-181.5 °C; ^{1}H NMR (400 MHz, $CDCl_3$) δ 0.91 (t, *J* = 6.8 Hz, 3H), 1.00-1.43 (m, 16H), 1.50 (quint, *J* = 7.17 Hz, 2H), 1.85 (quint, *J* = 7.0 Hz, 2H), 4.07 (t, *J* = 6.5 Hz, 2H), 5.14 (s, 2H), 7.00 and 7.16 (AB, *J* = 9.1 Hz, 4H), 7.28 (d, *J* = 8.7 Hz, 2H), 7.38-7.49 (m, 8H), 7.75 (d, *J* = 8.7 Hz, 2H), 8.17 (d, *J* = 8.9 Hz, 2H), 8.27 (d, *J* = 8.7 Hz, 2H); ^{13}C NMR (400 MHz, dept 135, $CDCl_3$) δ 14.6 (CH_3), 23.1 (CH_2), 26.4 (CH_2), 29.5 (CH_2), 29.8 (CH_2), 30.0 (CH_2), 30.1 (CH_2), 32.4 (CH_2), 68.8 (CH_2), 70.9 (CH_2), 114.9 (CH), 117.0 (CH), 122.6 (CH), 128.0 (CH), 128.8 (CH), 129.2 (CH), 129.5 (CH), 131.8, 132.3 (CH), 132.9 (CH); IR ν 1725 (C=O), 1258 (C−O) cm^{-1}; EI-HRMS, calcd. for $C_{46}H_{50}N_2O_6$ $[M]^+$ *m/z* 727.3747, found *m/z* 727.3783.

4-Benzoyloxybenzaldehyde 4-benzoyloxyphenylhydrazone (**1c**):

An Ar-flushed round bottom flask was charged with 4-benzoyloxybenzaldehyde (1.00 g, 4.42 mmol) and 4-benzoyloxyphenylhydrazine•HCl (1.17 g, 4.42 mmol) to which was added EtOH (25 mL) and stirred at 40 °C for 3 hrs. The reaction was then concentrated *in vacuo*. Purification was achieved by recrystallization in EtOH to obtain 6.16 g (93% yield) of hydrazone **1c** as light yellow crystals of a dull texture: mp 197.5-200.3 °C; ^{1}H NMR (400 MHz, $CDCl_3$) δ 7.14-7.17 (m, 4H), 7.24 (s, 1H), 7.50 and 7.54 (AB, *J* = 8.0 Hz, 4H), 7.62 and 7.66 (AB, *J* = 7.8 Hz, 2H), 7.71-7.75 (m, 4H), 8.21-8.23 (m, 4H); IR (thin film) ν 1731, 1267, 1196 cm^{-1}; EI-HRMS, calcd.

for $C_{27}H_{20}N_2O_4$ $[M]^+$ *m/z* 437.1501, found *m/z* 437.1519. Anal. Calcd for $C_{27}H_{20}N_2O_4$: C, 74.30; H, 4.62; N, 6.42. Found: C, 74.54; H, 4.70; N, 6.46.

Benzaldehyde α-chloroformyl-4-nitrophenylhydrazone (**2a**):[56]

Yield 93% from hydrazone **1a**[57]. Yellow solid: mp 168−170 °C [lit.23 mp 168 °C] (EtOH); 1H NMR (400 MHz, CDCl3) δ 7.38−7.47 (m, 4H), 7.53 (d, *J* = 8.9 Hz, 2H), 7.66 (d, *J* = 8.1 Hz, 2H), 8.45 (d, *J* = 8.9 Hz, 2H).

4-(4-(4-(Dodecyloxy)benzoyloxy)benzoyloxy)benzaldehyde α-chloroformyl-4-benzyloxyphenyl hydrazone (**2b**):

Hydrazone **1b** (1.05 g, 1.44 mmol) in DCM (7.5 mL) was treated with pyridine (0.14 mL, 1.7 mmol) and stirred under Ar at rt for 2 min. Triphosgene (427 mg, 1.44 mmol) was added at 0 °C and stirred for 5 min. after which the reaction was brought to rt and continued to stir for 3 hrs under Ar. The mixture was washed with 2% HCl followed by water, dried (Na_2SO_4), and evaporated. The crude product was than purified on a short column (DCM) to give 1.06 g (93% yield) of pure product as light yellow crystals: mp 185-186 °C (DSC); ^{1}H NMR (400 MHz, $CDCl_3$) δ 0.90 (t, *J* = 6.5 Hz, 3H), 1.10-1.43 (m, 16H), 1.49 (quint, *J* = 7.2 Hz, 2H), 1.84 (quint, *J* = 6.9 Hz, 2H), 4.06 (t, *J* = 6.5 Hz, 2H), 5.14 (s, 2H), 7.00 (d, *J* = 8.8 Hz, 2H), 7.15 and 7.19 (AB, *J* = 6.4 Hz, 4H), 7.28 (d, *J* = 8.3 Hz, 2H), 7.37-7.49 (m, 8H), 7.74 (d, *J* = 8.5 Hz, 2H), 8.16 (d, *J* = 8.8 Hz, 2H), 8.27 (d, *J* = 8.6 Hz, 2H); ^{13}C NMR (400 MHz, $CDCl_3$) δ 14.1, 22.6, 25.9, 29.0, 29.3, 29.5, 29.5, 29.6, 29.6, 31.9,68.3, 70.4, 114.4, 116.5, 120.8, 122.1, 126.5, 127.5, 128.3, 128.7, 129.0, 131.8, 132.4, 136.1, 155.5, 159.8, 163.8, 164.0, 164.2; IR ν 1723 (C=O), 1253 (C−O), 1157 (C−O), 748 (C−Cl) cm^{-1}; EI-HRMS, calcd. for $C_{47}H_{49}ClN_2O_7$ $[M+H]^+$ *m/z* 789.3307, found *m/z* 789.3301. Anal. Calcd for $C_{47}H_{49}ClN_2O_7$: C, 71.52; H, 6.26; N, 3.55; Cl, 4.49. Found: C, 71.61; H, 6.35; N, 3.63; Cl, 4.34.

4-Benzoyloxybenzaldehyde α-chloroformyl-4-benzoyloxyphenylhydrazone (**2d**):

Hydrazone **1c** (2.88 g, 6.60 mmol) in DCM (50 mL) was treated with Et_3N (1.10 mL, 7.92 mmol) and stirred under Ar at rt for 2 min. Triphosgene (979 mg, 3.30 mmol) was added at 0 °C and stirred for 5 min. after which time, the reaction was brought to rt and stirred for an additional 3 hrs under Ar. After the reaction was judged by TLC to be complete, the mixture was washed with 2% HCl followed by water, dried (Na_2SO_4), and evaporated. The crude orange-yellow crystalline product was than purified on a short column (DCM) to give 3.05 g (93% yield) of pure chloride as light yellow crystals: mp 177-179 °C (DSC); ^{1}H NMR (400 MHz, $CDCl_3$) δ 7.28 (d, *J* = 8.6 Hz, 2H), 7.36 (d, *J* = 8.7 Hz, 2H), 7.48-7.57 (m, 7H), 7.64-7.70 (m, 2H), 7.77 (d, *J* = 8.6 Hz, 2H), 8.20-8.24 (m, 4H); ^{13}C NMR (400 MHz, $CDCl_3$) δ 122.2, 123.9, 128.6, 128.7, 128.9, 129.1, 129.1, 130.2, 130.2, 130.9, 133.8, 134.0, 152.0, 152.8, 164.6, 164.7; IR ν 1728 (C=O), 1256 (C−O), 1199 (C−O), 1074 (C−O), 760 (C−Cl) cm^{-1}; EI-HRMS, calcd. for $C_{28}H_{19}ClN_2O_5$ $[M]^+$ *m/z* 499.1061, found *m/z* 499.1108; Anal. Calcd for $C_{28}H_{19}ClN_2O_5$: C, 67.41; H, 3.84; N, 5.61. Found: C, 67.17; H, 3.85; N, 5.68.

Tetrahydro-1,2,4,5-tetrazinan-3(2H)-ones **3a-3d**. General Procedure.

To a solution of carbamoyl chloride **2** (1.0 mmol) in DCM (15 mL), arylhydrazine or methylhydrazine (1.2 mmol) followed by Et_3N (2.4 mmol) were added. The resulting mixture was heated at 50 °C for 3 hrs and cooled to rt. For tetrazines **3a** and **3b**, the cooled reaction mixture was poured into 2% HCl and ice, and the resulting precipitation was filtered.

2-(4-Benzyloxyphenyl)-6-(4-nitrophenyl)-4-phenyltetrahydro-1,2,4,5-tetrazin-3(2H)-one (**3a**):[58]

Crude tetrazine was obtained in 72% yield and was partially purified by flash chromatography (SiO_2 washed with 1% Et_3N in hexanes, hexanes:CH_2Cl_2, 1:1) and used in the next step.

Analytical sample of **3a** was obtained by recrystallization from EtOH: mp 78−80 °C; ^{1}H NMR (400 MHz, CDCl3) δ 4.79 (d, *J* = 9.9 Hz, 1H), 4.87 (d, *J* = 10.2 Hz, 1H), 5.08 (s, 2H), 5.54 (t, *J* = 9.9 Hz, 1H), 7.00 (d, *J* = 9.1 Hz, 2H), 7.30−7.46 (m, 8H), 7.51 (d, *J* = 9.1 Hz, 2H), 7.52−7.59 (m, 2H), 7.95 (d, *J* = 9.4 Hz, 2H), 8.20 (d, *J* = 9.4 Hz, 2H); 13C NMR (400 MHz, $CDCl_3$) δ 70.2, 72.8, 114.9, 119.7, 124.1, 124.3, 126.3, 127.4, 128.0, 128.6, 129.0, 129.3, 134.4, 135.0, 136.7, 143.0, 147.7, 155.2, 156.5. Anal. Calcd for $C_{27}H_{23}N_5O_4$: C, 67.35; H, 4.81; N, 14.54. Found: C, 67.49; H, 4.84; N, 14.26.

2-(4-Carboxyphenyl)-6-(4-nitrophenyl)-4-phenyltetrahydro-1,2,4,5-tetrazin-3(2H)-one (**3d**):[58]

Obtained in 30% yield. Crude tetrazine was purified by washing with hot EtOAc: ^{1}H NMR (500 MHz, DMSO-d6) δ 5.47 (t, *J* = 8.9 Hz, 1H), 6.62 (d, *J* = 8.9 Hz, 1H), 6.69 (d, *J* = 8.8 Hz, 1H), 7.30−7.40 (m, 3H), 7.49 (d, *J* = 6.5 Hz, 2H), 7.76 (d, *J* = 8.9 Hz, 2H), 7.84 (d, *J* = 9.4 Hz, 2H), 7.92 (d, *J* = 8.9 Hz, 2H), 8.24 (d, *J* = 9.4 Hz, 2H). Anal. Calcd for $C_{21}H_{17}N_5O_5$: C, 60.14; H, 4.09; N, 16.70. Found: C, 59.88; H, 4.18; N, 16.74.

2-(4-Iodophenyl)-6-(4-nitrophenyl)-4-phenyltetrahydro-1,2,4,5-tetrazin-3(2H)-one (**3f**):[58]

Obtained in 90% yield as yellow solid using carbamoyl chloride **2a**, 4-iodophenylhydrazine and 1 equiv of Et_3N. Crude product was washed with warm EtOAc and recrystallized from EtOH: mp 197−200 °C; ^{1}H NMR (400 MHz, acetone-d6) δ 5.59 (t, *J* = 9.0 Hz, 1H), 6.09 (d, *J* = 9.1 Hz, 1H), 6.13 (d, *J* = 8.8 Hz, 1H), 7.22−7.32 (m, 3H), 7.47 (d, *J* = 8.9 Hz, 2H), 7.50−7.56 (m, Hz), 7.60 (d, *J* = 8.9 Hz, 2H), 7.89 (d, *J* = 9.4 Hz, 2H), 8.12 (d, *J* = 9.4 Hz, 2H); ^{13}C NMR (400 MHz, acetone-d6) δ 74.2, 118.9, 122.7, 123.9, 126.8, 128.4, 128.5, 137.0, 137.6, 142.3, 142.4, 148.5. Anal. Calcd for $C_{20}H_{16}IN_5O_3$: C, 47.92; H, 3.22; N, 13.97. Found: C, 47.75; H, 3.24; N, 13.70.

4-(4-Benzyloxyphenyl)-6-((4-(4-dodecyloxybenzoyloxy)benzoyloxy)phenyl)-2-methyltetrahydro-1,2,4,5-tetrazinan-3(2H)-one (**3v**):

To a round bottom flask charged with carbamoyl chloride **2b** (563 mg, 0.71 mmol) in DCM (10 mL) was added methylhydrazine (0.08 mL, 1.5 mmol). The mixture was stirred for 3 hrs at reflux, then washed with 2% HCl followed by water, dried (Na_2SO_4), and evaporated. The crude product was then purified by a Et_3N-pacified silica gel column (DCM:EtOAc, 5:1) yielding light pink crystals, which were further purified by recrystallization (EtOAc) to give 139 mg (24% yield) of pure product as white crystals: mp 177.4-179.8 °C; ^{1}H NMR (400 MHz, DMSO-d_6) δ 0.85 (t, J = 5.7 Hz, 3H), 1.23 (m, 16H), 1.41 (p, J = 5.7 Hz, 2H), 1.72 (m, 2H), 5.07 (s br, 2H), 5.11 (s br, 2H), 5.53 (m, 1H), 6.96 and 6.97 (AB, J = 6.4 Hz, 4H), 7.28 (d, J = 8.6 Hz, 2H), 7.36 (d, J = 7.2 Hz, 2H), 7.40-7.49 (m, 8H), 7.65 (d, J = 8.6 Hz, 2H), 8.02 (d, J = 8.8 Hz, 2H); EI-HRMS, calcd. for $C_{48}H_{54}N_4O_7$ $[M]^+$ *m/z* 799.4071, found *m/z* 799.4047.

4,6-bis(4-Benzoyloxyphenyl)-2-(thiophen-2-yl)tetrahydro-1,2,4,5-tetrazinan-3(2H)-one (**3h**):

Carbamoyl chloride **2d** (258 mg, 0.517 mmol) was added directly to crude 2-thiophenyl hydrazine (59.0 mg, 0.517 mmol) immediately after preparation of the hydrazine, and dissolved in 6.0 mL of a mixture of DCM:EtOH (1:1) to which was added Et_3N (0.08 mL, 0.569 mmol) and stirred under Ar for 3 hrs at 60 °C. The organic layer was washed with 1% HCl followed by water, dried (Na_2SO_4), and solvents were evaporated. Crude product was then purified on a short column pacified by adding a small portion of Et_3N to the silica slurry (DCM) resulted in 85.0 mg (29% yield) of **3h** as brown waxy solid: mp 160.8 °C dec; ^{1}H NMR (400 MHz, $CDCl_3$) δ 4.88 (d, J = 10.4 Hz, 1H), 5.01 (d, J = 10.4 Hz, 1H), 5.55 (dd, J = 8.3 Hz, 1H), 6.91 (s, 2H), 7.12 (s, 2H), 7.52-7.75 (m, 11H), 8.21 (m, 6H); EI-HRMS, calcd. for $C_{32}H_{24}N_4O_5S$ $[M]^+$ *m/z* 577.1546. Found: 577.1536. IR ν 1736 (C=O), 1264 (C−O) cm^{-1}.

4,6-bis(4-Benzoyloxyphenyl)-2-methyltetrahydro-1,2,4,5-tetrazinan-3(2H)-one (**3i**):

To a round bottom flask charged with carbamoyl chloride **2d** (500 mg, 1.00 mmol) in DCM (10 mL), was added methylhydrazine (0.12 mL, 2.21 mmol). The mixture was stirred for 3 hrs at reflux yielding an orange-white crude product, which was washed with 2% HCl followed by water, dried (Na_2SO_4), and solvents were evaporated. Purification of the crude product was then attempted on a silica gel column, which apparently resulted in the loss of the tetrazine product as no evidence of desired product was found in the eluent. Purification was then accomplished by chromatography using of Florisil® gel (Hexane:DCM (10:1)) yielding pale pink crystals, which were further purified by recrystallization (EtOAc) to give 335 mg (66% yield) of pure product as white crystals: mp 168.1-169.2 °C; ^{1}H NMR (400 MHz, $CDCl_3$) δ 3.27 (s, 3H), 4.60 (d, J = 10.3 Hz, 1H), 4.68 (d, J = 10.3 Hz, 1H), 5.29 (t, J = 10.3 Hz, 1H), 7.17 (d, J = 8.4 Hz, 3H), 7.26 (d, J = 7.4 Hz, 1H), 7.49-7.54 (m, 4H), 7.61-7.71 (m, 6H), 8.19 (d, J = 7.3 Hz, 4H); ^{13}C NMR (400 MHz, $CDCl_3$) δ 37.8, 69.8, 115.6, 121.3, 121.9, 123.0, 127.9, 128.5, 128.6, 129.2, 129.5, 130.1, 130.1, 132.9, 133.5, 133.8, 140.6, 147.0, 151.1, 153.6, 165.2, 165.4; IR (thin film) ν 1725 (C=O), 1634 (C−O), 1267 (C−O), cm^{-1}; EI-HRMS, calcd. for $C_{29}H_{25}N_4O_5$ $[M]^+$ *m/z* 509.1825; found 509.1819. Anal. Calcd for $C_{29}H_{25}N_4O_5$: C, 68.49; H, 4.76; N, 11.02. Found C, 68.25; H, 4.89; N, 11.01.

4,6-bis(4-Benzoyloxyphenyl)-2-phenyltetrahydro-1,2,4,5-tetrazin-3(2H)-one (**3j**):

To a round bottom flask charged with carbamoyl chloride **2d** (1.40 g, 2.81 mmol) dissolved in DCM (25 mL), was added phenylhydrazine (0.56 mL, 5.62 mmol). The mixture was stirred for 3 hrs at reflux, after which time, the reaction mixture was washed with 2% HCl followed by water, dried (Na_2SO_4), and evaporated. The crude product was then purified by a Et_3N-pacified silica gel column (DCM:EtOAc 10:1) yielding light yellow-orange crystals, which were further

purified by recrystallization (EtOH) to yield 1.02 g (64% yield) of white to light pink crystals of pure product: mp 109 °C dec; ^{1}H NMR (600 MHz, $CDCl_3$) δ 4.84 (d, *J* = 9.8 Hz 2H), 5.52 (m, *J* = 13.1 Hz, 1H), 6.98 (d, *J* = 8.2 Hz, 1H), 7.15 (t, *J* = 7.4 Hz, 1H), 7.21 (d, *J* = 7.7 Hz, 1H), 7.25 (m, 2H), 7.28 (d, *J* = 8.5 Hz, 1H), 7.32 (d, *J* = 8.6 Hz, 1H), 7.37 (t, *J* = 7.5 Hz, 1H), 7.41 (d, *J* = 8.6 Hz, 1H), 7.50-7.55 (m, 4H), 7.62-7.66 (m, 4H), 7.70 (d, *J* = 8.6 Hz, 1H), 7.75 (d, *J* = 7.7 Hz, 1H), 8.20 (dd, *J* = 8.3 Hz, 4H); ^{13}C NMR (400 MHz, $CDCl_3$) δ 113.5, 120.9, 121.4, 121.8, 122.3, 122.7, 123.4, 123.6, 123.9, 128.3, 128.5, 128.6, 128.6, 129.1, 129.3, 129.5, 129.8, 130.1, 130.2, 130.9, 133.7, 133.8, 136.2, 140.1, 142.2, 142.5, 148.7, 150.5, 151.3, 151.9, 152.2, 155.6, 155.8, 164.8; IR (thin film) ν 1737 (C=O), 1688 (C=O), 1264 (C−O), 1061 (C−O) cm^{-1}; EI-HRMS, calcd. for $C_{34}H_{26}N_4O_5$ $[M]^+$ *m/z* 571.1981, found *m/z* 571.2026. Anal. Calcd for $C_{34}H_{26}N_4O_5$: C, 71.57; H, 4.59; N, 9.82. Found: C, 71.44; H, 4.54; N, 9.68.

6-Oxoverdazyls **4a, 4d, 4f, 4i, 4j**. General Procedures.

Method A: A round bottom flask was charged with tetrazine **3** (0.5 mmol), $K_3Fe(CN)_6$ (3 mmol), 0.5 M Na_2CO_3 (10 mL), cat. $[NBu_4]^+Br^-$ (10−20 mol %) and DCM (10 mL). The mixture was vigorously stirred at rt for 2−8 hrs until tetrazine **3** is no longer visible on TLC, after which time the reaction mixture was washed with 2% HCl and separated, dried (Na_2SO_4), and evaporated. The crude product was purified by column chromatography (DCM:EtOAc, 10:1) followed by recrystallization to give the desired verdazyl as purple crystals.

Method B: A mixture of tetrazine **3** (0.216 mmol), CH_2Cl_2 (5 mL), H_2O (5 mL), $NaIO_4$ (0.238 mmol), and $[NBu_4]^+Br^-$ or $[NEt_4]^+Br^-$ (10−20 mol %) was stirred overnight at rt. The organic layer was separated, and radical **4** was isolated and purified as in Method A.

Method C: A mixture of purified tetrazine **3** (1.50 mmol), anhydrous Na_2CO_3 (15.0 mmol), PbO_2 (30.0 mmol) in a solution of toluene (6 mL) and MeCN (3 mL) was stirred for 18-24 hrs at rt. The reaction mixture was filtered, washed with 2% HCl, and then purified by a silica gel column (CH_2Cl_2:EtOAc, 10:1) followed by recrystallization to give the desired verdazyl as a purple solid.

1-(4-Benzyloxyphenyl)-5-(4-nitrophenyl)-3-phenyl-6-oxoverdazyl (**4a**).[58]

Method A, yield 86%; Method B, yield 96%. Dark purple-brown crystals: mp 167−169 °C (MeCN); UV−*vis* (dioxane) λmax (log ε) 359 (3.97), 475 (3.49), 579 (3.53). Anal. Calcd for $C_{27}H_{20}N_5O_4$: C, 67.77; H, 4.21; N, 14.64. Found: C, 67.88; H, 4.28; N, 14.72.

Attempted Preparation of 1-(4-Carboxyphenyl)-5-(4-nitrophenyl)-3-phenyl-6-oxoverdazyl (**4d**):[58]

Tetrazine **3d** (100 mg) was oxidized according to Method B in the presence of stoichiometric amounts of Na_2CO_3. After 2 hrs TLC analysis demonstrated nearly complete conversion of **3d**. The red-brown reaction mixture was carefully acidified with 1% HCl, the CH_2Cl_2 layer was separated, and the aqueous layer was extracted with ether. The combined organic extracts were dried (Na_2SO_4), and solvent was evaporated. The residue (30 mg) was separated on a short silica gel column (CH_2Cl_2:MeCN, 5:1) to give 4 mg of a red-wine solid mixture of 3 products with similar polarity and containing the expected radical **4d**: ESI-HRMS TOF, calcd. for $C_{21}H_{14}N_5O_5$ [M]+ *m/z* 416.1000, found *m/z* 416.0995. Oxidation of **3d** with PbO_2 in hot AcOH (10 min), followed by usual workup and chromatographic separation gave **4d** in 12% yield as a red-wine solid, which slowly decolorized.

1-(4-Iodophenyl)-5-(4-nitrophenyl)-3-phenyl-6 oxoverdazyl (**4f**).[58]

Method A; yield 85%. Dark purple-brown crystals: mp >260 °C (EtOAc). Anal. Calcd for $C_{20}H_{13}IN_5O_3$: C, 48.21; H, 2.63; N, 14.06. Found: C, 48.07; H, 2.63; N, 13.93.

1,3-bis(4-Benzoyloxyphenyl)-5-methyl-6-oxoverdazyl (**4i**):

Oxidation using *Method C* obtained 80.3 mg of the radical (22% yield) as a deep red wax over 8 hours. Oxidation was stopped short of the normal 18-24 hrs since it was noted that as oxidation proceeded, there was a concomitant loss of the verdazyl, presumably through disproportionation. It was also noted that when verdazyl **4i** was re-dissolved with no other reagents present, loss of the verdazyl was also observed although slower than under chemically oxidative conditions. Method A led to decomposition. EI-HRMS, calcd. for $C_{29}H_{21}N_4O_5$ $[M]^+$ *m/z* 506.1545, found *m/z* 506.1585.

1,3-bis(4-Benzoyloxyphenyl)-5-phenyl-6-oxoverdazyl (**4j**):

Method A: followed by recrystallization (MeCN:EtOAc, 10:1) gave 4.42 g (81% yield) of the desired verdazyl as purple crystals. Method C: followed by recrystallization (MeCN:EtOAc, 10:1) gave 514 mg (57% yield) of the desired verdazyl as a purple solid: mp 194.1-195.8 °C; IR (thin film) ν 1729 (C=O), 1687 (C=O), 1259 (C−O) cm^{-1}; EI-HRMS, calcd. for $C_{34}H_{23}N_4O_5$ $[M+Na]^+$ *m/z* 590.1566, found *m/z* 590.1553. Anal. Calcd for $C_{34}H_{23}N_4O_5$: C, 71.95; H, 4.08; N, 9.87. Found: C, 71.26; H, 4.09; N, 9.57.

1-(4-Benzyloxyphenyl)-5-(4-benzamidophenyl)-3-phenyl-6-oxoverdazyl (**4b**):[58]

A suspension of PtO_2 (25 mg, 0.1 mmol) in EtOH (150 mL) was hydrogenated in a hydrogenator for 15 min at 50 psi after being purged from oxygen three times. A solution of crude **4a** (522 mg, 1.1 mmol) in THF (35 mL) was added and hydrogenated with H_2 for 2 hrs until starting material

disappeared. The reaction was then exposed to air. A color change from colorless to dark purple was observed indicating *leuco* to verdazyl transformation. The mixture was passed through Celite, and solvents were evaporated to give 400 mg (82% yield) of dark blue-purple crude product: HRMS-TOF, calcd for $C_{27}H_{22}N_5O_2$ $[M + H]^+$ *m/z* 448.1768, found *m/z* 448.1770. To the crude amino- intermediate (470 mg, 1.0 mmol) in CH_2Cl_2 (15 mL) was added benzoyl chloride (1.0 mmol) and Et_3N (1.2 mmol), and the mixture was stirred for 2 hrs at rt. The mixture was washed with 5% HCl and extracted (CH_2Cl_2), organic layers were dried (Na_2SO_4), and solvent was evaporated. A crude product was oxidized (Method A) and purified by column chromatography (SiO_2, CH_2Cl_2) to give 400 mg (67% yield) of amide **4b** as black purple crystals: mp 233−234 °C dec (EtOH then MeCN); HRMS, calcd for $C_{34}H_{27}N_5O_3$ $[M + H]^+$ *m/z* 553.2108, found *m/z* 553.2101. Anal. Calcd for $C_{34}H_{26}N_5O_3$: C, 73.90; H, 4.74; N, 12.67. Found: C, 73.15; H, 4.77; N, 12.45.

1-(4-Benzoyloxyphenyl)-5-(4-benzamidophenyl)-3-phenyl-6-oxoverdazyl (**4c**):[58]

To a solution of 10% Pd/C (29 mg) in 10 mL of EtOH was added a solution of **4b** (103 mg. 0.19 mmol) in 7.5 mL of THF in a hydrogenator flask. The mixture was purged from oxygen three times and was then hydrogenated with H_2 at 50 psi for 24 hrs. An equal portion of 10% Pd/C was then added to the mixture, which was subsequently repurged three times, and hydrogenation was continued for another 24 h. The mixture was oxidized with air, solvents were evaporated, and the residue was passed through silica gel (CH_2Cl_2:EtOAc, 10:1) to give the phenol intermediate (58 mg, 57% yield) as a deep purple solid: mp 104 °C, dec; HRMS-TOF, calcd for $C_{27}H_{24}N_5O_3$ $[M + H]^+$ *m/z* 466.1874, found *m/z* 466.1884. To a crude mixture of the phenolic intermediate (75 mg, 0.13 mmol) in CH_2Cl_2 (3 mL) was added benzoyl chloride (0.13 mmol) and Et_3N (0.15 mmol), and a mixture was stirred for 2 hrs at rt. The mixture was washed with 5% HCl and extracted

(CH_2Cl_2), organic layers were dried (Na_2SO_4), solvent was evaporated, and the crude product was purified by column chromatography (SiO_2, CH_2Cl_2) to give 60 mg (74% of yield) of ester **4c** as dark purple crystals, which were recrystallized from MeCN, followed by EtOAc: mp 265 °C (dec). Anal. Calcd for $C_{34}H_{24}N_5O_4$: C, 72.07; H, 4.27; N, 12.36. Found: C, 71.78; H, 4.41; N, 12.47.

1,3-bis(4-Hydroxyphenyl)-5-phenyl-6-oxoverdazyl (**4k**):

A round bottom flask was charged with verdazyl **4j** (126 mg, 0.22 mmol), DCM (5.0 mL), and 0.1 M KOH/MeOH (5.5 mL). The mixture was stirred vigorously for 20 min at rt and then quenched with 18% HCl (5.0 mL). The organic layer was washed with water and extracted with a large portion of EtOAc. The verdazyl diol was purified on a silica-gel plug (DCM:EtOAc, 8:1), dried (Na_2SO_4), followed by evaporation (cold bath) to reveal 74.6 mg (93% yield) as black crystals: mp 179.5-180.9 °C; IR (thin film) ν 3361 (O−H), 1729 (C=O), 1212 (C−O), 1042 (C−O) cm^{-1}; EI-HRMS, calcd. for $C_{20}H_{15}N_4O_3$ $[M]^+$ *m/z* 360.1207, found *m/z* 360.1222.

Esterification of **4k**. General procedures.

Method D: To a round bottom flask charged with verdazyl **4k** (0.14 mmol) and 4-substituted benzoic acid[67-72] (0.31 mmol) was added DCC (0.42 mmol) and DMAP (0.03 mmol) in EtOAc (5.0 mL). The reaction was stirred overnight, the undissolved urea solids were filtered off, and the mixture washed with 2% HCl followed by water, dried (Na_2SO_4), and solvents evaporated. The crude verdazyl was purified on a silica-gel column (DCM → DCM:EtOAc, 8:1) and then recrystallized (MeCN:EtOAc, 6:1) to give pure product as deep purple crystals.

Method E: A round bottom flask was charged with 4-substituted benzoic acid[67-72] (0.65 mmol) in DCM (10.0 mL) along with 2 drops of DMF was stirred at 0 °C under Ar. Oxalyl chloride (1.9

mmol) was added dropwise to this suspension and stirred at 0 °C for 2 min and then brought to rt and continued to stir for 15 min. while noting the disappearance of undissolved starting material as it was converted to the acid chloride. The solvent was removed *in vacuo* with a cold trap; the crystals were dried on a pump for 30 min at 40 °C. The white to orange crystals were brought to rt and re-dissolved in DCM (3.0 mL) to which Et_3N (0.648 mmol) was added followed by the verdazyl diol **4k** (0.648 mmol) under Ar and stirred for 30 min. After the reaction was determined to be complete by TLC, it was washed with 2% HCl followed by water, dried (Na_2SO_4), and solvents evaporated. The crude verdazyl was purified on a silica-gel column (DCM → DCM:EtOAc, 8:1) and then recrystallized (MeCN:EtOAc, 6:1) giving the desired verdazyl as deep purple crystals.

1,3-bis(4-(4-(Decyloxy)benzoyloxy)benzoyloxy)-5-phenyl-6-oxoverdazyl (**4m**):

Method D, 112 mg (72% yield) of pure product **4m** as purple crystals: mp 127.3-128.4 °C; EI-HRMS, calcd. for $C_{68}H_{71}N_4O_{11}$ $[M]^+$ *m/z* 1120.5198, found *m/z* 1120.5211. Anal. Calcd for $C_{68}H_{71}N_4O_{11}$: C, 72.90; H, 6.39; N, 5.00. Found C, 73.14; H, 6.32; N, 4.96.

1,3-bis(4-(4-(Dodecyloxy)benzoyloxy)benzoyloxy)-5-phenyl-6-oxoverdazyl (**4n**):

Method E, 106 mg (65% yield): mp 121 °C; EI-HRMS, calcd. for $C_{72}H_{79}N_4O_{11}$ $[M]^+$ *m/z* 1176.5824, found *m/z* 1176.5868; Anal. Calcd for $C_{72}H_{79}N_4O_{11}$: C, 73.51; H, 6.77; N, 4.76. Found: C, 73.60; H, 6.67; N, 4.74.

1,3-bis(4-(4-(Tetradecyloxy)benzoyloxy)benzoyloxy)-5-phenyl-6-oxoverdazyl (**4o**):

Method E, 294 mg (74% yield) of **4o**: mp 118 °C; IR (thin film) ν 1738 (C=O), 1260 (C−O), 1062 (C−O) cm^{-1}; EI-HRMS, calcd. for $C_{76}H_{87}N_4O_{11}$ $[M]^+$ *m/z* 1232.6450, found: 1232.6489; Anal. Calcd for $C_{76}H_{87}N_4O_{11}$: C, 74.06; H, 7.12; N, 4.55. Found: C, 73.81; H, 7.21; N, 4.47.

1,3-bis(4-(4-(Hexadecyloxy)benzoyloxy)benzoyloxy)-5-phenyl-6-oxoverdazyl (**4p**):

Method E, 167 mg (69% yield): mp 91.1-93.3 °C; IR ν 1701 (C=O), 1259 (C−O), 1041 (C−O). EI-HRMS, calcd. for $C_{80}H_{95}N_4O_{11}$ $[M]^+$ *m/z* 1288.7076. Found: 1288.7091. Anal. Calcd for $C_{80}H_{95}N_4O_{11}$: C, 74.56; H, 7.43; N, 4.35. Found: C, 74.29; H, 7.42; N, 4.28.

1,3-bis(4-((4-(Dodecyloxy)benzoyloxy)diazenyl)benzoyloxy phenyl)-5-phenyl-6-oxoverdazyl (**4q**):

Method E, 163 mg (65%): mp 139.85-141.75 °C; IR ν 1737 (C=O), 1258 (C−O). EI-HRMS, calcd. for $C_{70}H_{79}N_8O_7$ $[M]^+$ *m/z* 1144.6150, found: 1144.6180. Anal. Calcd for $C_{70}H_{79}N_8O_7$: C, 73.46; H, 6.96; N, 9.79. Found: C, 73.19; H, 6.94; N, 9.67.

1,3-bis(4-(4-(dodecyloxy)benzyloxy)benzoyloxy)-5-phenyl-6-oxoverdazyl (**4r**):

Method D, 148 mg (51%): mp 86.44-97.54 °C; EI-HRMS, calcd. for $C_{72}H_{83}N_4O_9$ $[M]^+$ *m/z* 1148.6238, found: 1148.6594.

1,3-bis(4-((4-(dodecyloxy)benzoyloxy)acryloyl)-5-phenyl-6-oxoverdazyl (**4s**):

Method C, 103 mg (41%): mp 90.79-97.61 °C. IR ν 1729.71, 1602.00, 1132.55. EI-HRMS, calcd. for $C_{62}H_{75}N_4O_7$ $[M]^+$ *m/z* 988.5714. Found: 988.5710. Anal. Calcd for $C_{62}H_{75}N_4O_7$: C, 75.35; H, 7.65; N, 5.67. Found: C, 75.32; H, 7.95; N, 5.02.

1,3-bis(4-(4-(dodecyloxy)benzoyloxy)1,1'-biphenyl]-4-carboxylate)-5-phenyl-6-oxoverdazyl (**4t**):

Method D, 81.7 mg (54%): mp decomposition noted at 120.2 °C. $[M]^+$ *m/z* 1088.5982. Found: 1088.6022. Anal. Calcd for $C_{62}H_{75}N_4O_7$: C, 77.25; H, 7.32; N, 5.15. Found C, 76.14; H, 7.66; N, 4.38.

4,6-bis(4-Benzoyloxyphenyl)-2-phenyl-1,2,4,5-tetrazin-3(2H)-one (**5j**):

Verdazyl **4j** (15.0 mg, 0.026 mmol) and Pd/C (1.0 mg, 0.02 mmol) in deuterated chloroform (1.0 mL) were added to an NMR tube and bubbled with Ar for 5 min. The mixture was then bubbled with H_2 at atmospheric pressure and the tube periodically capped and inverted to simulate stirring, followed by re-subjecting the mixture to H_2 until the deep purple solution became colorless, whereupon the tube was capped and sealed with a PARAFILM® wrap: NMR analysis revealed two tautomers with signals common to both: ^{1}H NMR (600 MHz, $CDCl_3$) δ 7.18 (d, J = 8.4 Hz, 1H), 7.23 (d, J = 9.4 Hz, 1H), 7.28 (d, J = 7.0 Hz, 2H), 7.34 (t, J = 8.0 Hz, 1H), 7.38 (t, J = 7.8 Hz, 1H), 7.45-7.49 (m, 4H), 7.59-7.64 (m, 3H), 7.70 (d, J = 8.6 Hz, 2H), 7.77 (d, J = 9.4 Hz, 1H), 8.01 (d, J = 7.0 Hz, 2H), 8.13-8.17 (m, 4H). Signals unique to each tautamer: 6.08 (s, 0.5H), 6.12 (s, 1H), 7.13 (t, J = 7.1 Hz, 0.5 H), 7.22 (m, 0.5H, underneath a doublet at 7.23).

4-(4-(4-(Dodecyloxy)benzoyloxy)benzoyloxy)benzaldehyde (**7a**):[64]

A flask was charged with 4-((4-(dodecyloxy)benzoyloxy)benzoic acid[67] (470 mg, 1.1 mmol) in DCM (8 mL) along with 2 drops of DMF and stirred at 0 °C under Ar. Thionyl chloride (0.8 mL, 11.0 mmol) was added dropwise to this mixture and stirred at 0 °C for 2 min and then brought to rt and continued to stir for 1 hr. The solvent was evaporated using a water aspirator and cold trap, and the crystals were dried on a pump for 30 min at 40 °C. The white crystals were brought to rt and re-dissolved in DCM (5.0 mL). Et_3N (0.15 mL, 1.1 mmol) and *p*-hydroxybenzaldehyde (135 mg, 1.1 mmol) were sequentially added to the stirred solution under Ar. The reaction was determined to be complete by TLC after 30 min. It was then washed with 2% HCl followed by water, dried (Na_2SO_4), and evaporated. The crude product was purified on a silica-gel column (DCM) and then recrystallized (EtOAc) giving 549 mg (94% yield) of the desired aldehyde as white crystals: mp 99.3-101.5 °C; ^{1}H NMR (400 MHz, $CDCl_3$) δ 0.88 (t, J = 6.8 Hz, 3H), 1.22-

1.42 (m, 16H), 1.44-51 (m, 2H), 1.83 (quint, J = 7.0 Hz, 2H), 4.05 (t, J = 6.6 Hz, 2H), 6.99 (d, J = 8.9 Hz, 2H), 7.38-7.44 (m, 4H), 7.98 (d, J = 8.6 Hz, 2H), 8.15 (d, J = 8.9 Hz, 2H), 8.28 (d, J = 8.8 Hz, 2H), 10.03 (s, 1H); ^{13}C NMR (100 MHz, DEPT 135, $CDCl_3$) δ 14.5 (CH_3), 23.1 (CH_2), 26.4 (CH_2), 29.5 (2xCH_2), 29.8 (2 × CH_2), 29.96, 29.99 (CH_2), 30.06, 30.4 (CH_2), 31.3, 32.3 (CH_2), 114.85 (CH), 122.7 (CH), 123.0 (CH), 131.7 (CH), 132.3 (CH), 132.8 (CH), 138.5 (CH), 191.3 (CH); IR (thin film) ν 2841 (CHO), 1731 (C=O), 1259 (C−O) cm^{-1}; EI-HRMS, calcd. for $C_{33}H_{38}O_6$ $[M]^+$ *m/z* 531.2747, found *m/z* 531.2762.

Di-tert-butyl 1-(thiophen-2-yl)hydrazine-1,2-dicarboxylate (**8a**):

To a solution of thiophene (1.9 mL, 23.8 mmol) in THF (3 mL) was added *t*-BuLi (17.4 mL, 1.7 M in pentane, 26.2 mmol) under Ar at -78 °C. After 1.5 hrs of stirring, a THF (20 mL) solution of di-*tert*-butyl-azodicarboxylate (DTBAD) (6.02 g, 26.2 mmol) was added dropwise. The mixture was stirred at -78 °C for 0.5 hrs, then 1 hr at rt, and quenched with water. The organic products were extracted (EtOAc), the extracts dried (Na_2SO_4), the solvents evaporated, and the light orange residue was passed through a short silica-gel column (hexane/DCM followed by DCM) to give 6.938 g (93% yield) of the hydrazide as a yellow to light brown solid: mp 162.6-162.8 °C; ^{1}H NMR (400 MHz, $CDCl_3$) δ 1.50 (s, 9H), 1.52 (s, 9H), 6.76-6.84 (m, 2H), 6.92 (s, 1H); EI-HRMS, calcd. for $C_{14}H_{22}N_2O_4S$ $[M+Na]^+$ *m/z* 337.1198, found *m/z* 337.1192. Anal. Calcd for $C_{14}H_{22}N_2O_4S$: C, 53.48; H, 7.05; N, 8.91. Found C, 53.69; H, 6.99; N, 8.76.

Thiophen-2-ylhydrazine (**9a**):

A solution of hydrazide (447 mg, 0.52 mmol) in DCM (7 mL) was rapidly added to a solution of TfOH (0.23 mL, 2.58 mmol) in CF_3CH_2OH (3 mL) at 0 °C under Ar. The mixture was vigorously stirred for 2 min. Separation of the desired organic products was achieved with a

cold solution of DCM (5 mL) and sat. $NaHCO_3$ (10 mL) followed by extraction of products from the aqueous layer (2 ×). Extracts were then dried (Na_2SO_4) and the solvents evaporated in a cold bath to give crude 2-thiophenyl hydrazine as a viscous, yellow to orange oil (52.5 mg, 89%) that darkened upon standing (30 min). ^1H NMR (400 MHz, $CDCl_3$) δ 4.06 (s, 1H), 4.94 (br s, 2H), 6.47 (s, 1H), 6.55 (s, 1H).

REFERENCES

1. Reinitzer, F. Beitrage zur kenntniss des cholesterins. *Monatshefte für Chemie (Wien)*, **1888**, *9*, 421–441.

2. Collings, P. J.; Hird, M. *Introduction to liquid crystals: chemistry and physics*; Taylor & Francis Ltd: London, 1997.

3. Reddy, R. A; Tschierske, C. Bent-core liquid crystals: polar order, superstructural chirality and spontaneous desymmetrisation in soft matter systems. *J. Mater. Chem*., **2006**, *16*, 907–961.

4. Tschierske, C. Micro-segregation, molecular shape and molecular topology – partners for the design of liquid crystalline materials with complex mesophase morphologies. *J. Mater. Chem*., **2001**, *11*, 2647-2671.

5. Dantlgraber, G.; Baumeister, U.; Diele, S.; Kresse, H.; Luhmann, B.; Lang, H.; Tschierske, C. Evidence for a new ferroelectric switching liquid crystalline phase formed by a carbosilane based dendrimer with banana-shaped mesogenic units. *J. Am. Chem. Soc*. **2002**, *124*, 14852-14853.

6. Lagerwall, S. T. *Ferroelectric and antiferroelectric liquid crystals*; Wiley VCH, Weinheim, 1999.

7. Nadasi, H.; Weissflog, W.; Eremin, A.; Pelzl, G.; Diele, S.; Das, B.; Grande, S. Ferroelectric and antiferroelectric ‘‘banana phases’’ of new fluorinated five-ring bent-core mesogens. *J. Mater. Chem*., **2002**, *12*, 1316–1324.

8. Wirth, I.; Diele, S.; Eremin, A.; Pelzl, G.; Grande, S.; Kovalenko, L.; Pancenkoa, N.; Weissflog, W. New variants of polymorphism in banana-shaped mesogens with cyano-substituted central core. *J. Mater. Chem*., **2001**, *11*, 1642-1650.

9. C. A. Hunter, C. A.; Sanders, J. K. M. The nature of π-π interactions. *J. Am. Chem. Soc*., **1990**, *112*, 5525-5534.

10. Bedel, J. P.; Rouillon, J. C.; Marcerou, J. P.; Laguerre, M.; Achard, M. F.; Nguyen, H. T. Physical characterization of B1 and B2 phases in a newly synthesized series of banana shaped molecules. *Liq. Cryst*., **2000**, *27*, 103-113.

11. Neuvonen, H.; Neuvonen, K.; Pasanen, P. Evidence of substituent-induced electronic interplay: effect of the remote aromatic ring substituent of phenyl benzoates on the sensitivity of the carbonyl unit to electronic effects of phenyl or benzoyl ring substituents. *J. Org. Chem*., **2004**, *69*, 3794-3800.

12. Reddy, R. A.; Sadashiva, B. K. Influence of fluorine substituent on the mesomorphic properties of five-ring ester banana-shaped molecules. *Liq. Cryst*., **2003**, *30*, 1031-1050.

13. Dantlgraber, G.; Shen, D.; Diele, S.; Tschierske, C. Antiferroelectric switchable mesophases of nonchiral bent-core liquid crystals containing fluorinated central cores. *Chem. Mater*., **2002**, *14*, 1149-1158.

14. Reddy, R. A.; Sadashiva, B. K. Ferroelectric properties exhibited by mesophases of compounds composed of achiral banana-shaped molecules. *J. Mater. Chem*., **2002**, *12*, 2627-2632.

15. Reddy, R. A.; Raghunathan, V. A.; Sadashiva, B. K. Novel ferroelectric and antiferroelectric smectic and columnar mesophases in fluorinated symmetrical bent-core compounds. *Chem. Mater*., **2005**, *17*, 274-283.

16. Pelzl, G.; Weissflog, W. *Thermotropic liquid crystals: recent advances*., Ramamoorthy A., Ed.: Springer, The Netherlands, 2007, 1-79.

17. Nakata, M.; Link, D. R.; Araoka, F.; Thisayukta, J.; Takanishi, Y.; Ishikawa, K.; Watanabe J.; Takezoe, H. A racemic layer structure in a chiral bent-core ferroelectric liquid crystal. *Liq. Cryst*., **2001**, *28*, 1301-1308.

18. Shen, D.; Pegenau, A.; Diele, S.; Wirth, I.; Tschierske, C. Molecular design of nonchiral bent-core liquid crystals with antiferroelectric properties. *J. Am. Chem. Soc*., **2000**, *122*, 1593-1601.

19. Eremin, A.; Nadasi, H.; Pelzl, G.; Diele, S.; Kresse, H.; Schmalfuss, H.; Wirth, I.; Weissflog, W.; Grande, Paraelectric–antiferroelectric transitions in the bent-core liquid-crystalline materials. S. *Phys. Chem. Chem. Phys*., **2004**, *6*, 1290-1298.

20. Avarvari, N.; Wallis J. D. Strategies towards chiral molecular conductors. *J. Mater. Chem*., **2009**, *19*, 4061-4076.

21. Yakhmi, J. V. Molecule-based magnets. *B Mater. Sci*., **2009**, *32*, 217-225.

22. Tamura, R.; Uchida, Y.; Suzuki, K. *Nitroxides: Theory, experiment and applications*. Kokorin A.I.: InTech, 2012, p. 191-201.

23. Dvolaitzky, M.; Billard, J.; Poldy, F. Smectic E, C and A free radicals. *Tetrahedron*, **1976**, *32*, 1835-1838.

24. Zheng, M.Y.; An Z.W. Rod-like schiff base magnetic liquid crystals bearing organic radical. *Chin. J. Chem*., **2006**, *24*, 1754-1757.

25. Uchida, Y.; Ikuma, N.; Tamura, R.; Shimono, S.; Noda, Y.; Yamauchi, J.; Aokic, Y.; Nohira, H. Unusual intermolecular magnetic interaction observed in an all-organic radical liquid crystal *J. Mater. Chem*., **2008**, *18*, 2950-2952.
26. Neugebauer, F. A. Hydrazidinyl radicals: 1,2,4,5- tetraazapentenyls, verdazyls, and tetrazolinyls. *Angew. Chem. Int. Ed. Engl*., **1973**, *12*, 455-464.

27. Hicks, R. G. The 2003 CSC Pure or applied inorganic chemistry award lecture adventures in stable radical chemistry. *Can. J. Chem.*, **2004**, *82*, 1119-1127.

28. Goldschmidt, S.; Renn K. Zwei-wertiger stickstoff aber das a,a-diphenyl-8-trinitrophenyl-hydrazyl. *Ber. Deutsch*. *Chem. Gesel*., **1922**, *B55*, 628-643.

29. Mukai, K.; Hatanaka, T.; Senba, N.; Nakayashiki, T.; Misaki, Y.; Tanaka, K.; Ueda, K.; Sugimoto, T.; Azuma, N. Magnetic semiconductor: structural, magnetic, and conducting properties of the salts of the 6-oxoverdazyl radical cation with M(dmit)2 anions (M = Ni, Zn, Pd, and Pt, dmit = 1,3-dithiol-2-thione-4,5-dithiolate). *Inorg. Chem*., **2002**, *41*, 5066-5074.

30. Neugebauer, F. A.; Fischer, H.; Siegel, R. 6-Oxo- und 6-thioxoverdazyle. *Chem. Ber*. **1988**, *121*, 815-822.

31. Mukai, K.; Shikata, H.; Azuma, N.; Kuwata, K. ELDOR studies of 1,3,5-triphenylverdazyl and 1,5-diphenyl-3-(4-chlorophenyl)verdazyl radicals. *J. Mag. Reson*. **1979**, *35*, 133-137.

32. Neugebaur, F. A.; Trischmann, H.; Taigel, G. NMR-spektren yon verdazylen. *Monatsh. Chem.* **1967**, *98*, 713-725.

33. Gilroy, J. B.; McKinnon, S. D. J.; Kennepohl, P.; Zsombor, M. S.; Ferguson, M. J.; Thompson, L. K.; Hicks, R. G. Probing electronic communication in stable benzene-bridged verdazyl diradicals. *J. Org. Chem*., **2007**, *72*, 8062-8069.

34. Hicks, R. G. *Stable Radicals: Fundamentals and applied aspects of odd-electron compounds*, Hicks RG, Ed.: Wiley, UK, 2010, p. 245-273.

35. Koivisto, B. D.; Hicks R. G. Strong ferromagnetic metal-ligand exchange in a nickel bis(3,5-dipyridylverdazyl) complex. *Coord. Chem. Rev*., **2005**, *249*, 2612-2630.

36. Neugebauer, F. A.; Fischer H., Krieger C. EPR and ENDOR studies of 6-oxo- and 6-thioxoverdazyls. X- ray molecular structure of 1,3,5-triphenyl-6-oxoverdazyl and 3-tert-butyl-1,5-diphenyl-6-thioxoverdazyl. *J. Chem. Soc. Perkin Trans*. **1993**, *2*, 535-544.

37. Rayner, G.; Smith, T.; Barton, W.; Newton, M.; Deeth, R. J.; Prokes, I.; Clarkson, G. J.; Haddleton, D. M. A comparison of verdazyl radicals modified at the 3-position as mediators in the living radical polymerisation of styrene and n-butyl acrylate. *Polym. Chem*., **2012**, *3*, 2254–2260.

38. Williams, D. E. Crystal structure of 2,4,6-triphenylverdazyl. *Acta Cryst*. **1973**, *B29*, 96-102.

39. Nakatsuji, S.; Kitamura, A.; Takai, A.; Nishikawab, K.; Morimotob, Y.; Yasuokab, N.; Kawamura, H.; Anzai, H. CT Complexes Derived from Verdazyl Radicals. *Z. Naturforsch*., **1998**, *B53*, 495-502.

40. Kuhn, R.; Trischmann, H. Über verdazyle, eine neue klasse cyclischer N-haltiger radikale. *Monatsh. Chem*., **1964**, *95*, 457-479.

41. Nesterenko, A. M.; Polumbrik, O. M.; Markovskii, L. N. Electronic and spatial structure of leucoverdazyls. *Zh. Org. Khim*., **1978**, *14*, 1332-1335.

42. Miura, Y.; Morimoto, Y.; Kinoshita, M. Reaction of a stable free nitrogen-centered radical, 3,4-Dihydro-2,4,6-triphenyl-2H-1,2,4,5-tetrazin-1-yl, with Grignard Reagents. *Chem. Soc. Jpn*., **1976**, *49*, 253-255.

43. Öhrström, L. Can DFT calculations help the molecular designer to construct molecule based magnetic materials?. *C. R. Chimie.*, **2005**, *8*, 1374-1385.

44. Luneau, D. Molecular magnets. *Curr. Opin. Solid St. Mater.*, **2001**, *5*, 123-129.

45. Gavezzotti, A. Are crystal structures predictable?. *Acc. Chem. Res.*, **1994**, *27*, 309-314.

46. Desiraju, G. R. Supramolecular synthons in crystal engineering—a new organic synthesis. *Angew. Chem. Int. Ed. Engl*., **1995**, *34*, 2311-2327.

47. Coey, J. M. D. *Magnetism and magnetic materials*, Cambridge University Press, New York, 2010.

48. Hicks, R.G.; Lemaire, M. T.; Öhrström, L.; Richardson, J. F.; Thompson, L. K.; Xu, Z. Strong supramolecular-based magnetic exchange in π-stacked radicals- structure and magnetism of a hydrogen-bonded verdazyl radical: hydroquinone molecular solid. *Am. Chem. Soc*., **2001**, *123*, 7154.

49. Jankowiak, A.; Pociecha, D.; Monobe, H.; Szczytko, J.; Kaszynski, P. Thermochromic discotic 6-oxoverdazyls. *Chem. Commun*., **2012**, *48*, 7064–7066.

50. Jankowiak, A.; Pociecha, D.; Monobe, H.; Szczytko, J.; Kaszynski, P. Photoconductive liquid-crystalline derivatives of 6-oxoverdazyl. *J. Am. Chem.Soc*. **2012**, *134*, 2465−2468.

51. Jasinski, M.; Pociecha, D.; Monobe, H.; Szczytko, J.; Kaszyński, P. Tetragonal phase of 6-oxoverdazyl bent-core derivatives with photoinduced ambipolar charge transport and electrooptical effects. *J. Am. Chem. Soc*. **2014**, *136*, 14658−14661.

52. Lydon, J.E.; Hanna, J. *Liquid crystalline semiconductors: materials, properties and applications*. Bushby RJ, Kelly SM, O'Neill M.: Ed. Springer, UK. 2013, p. 1-61.

53. Alberola, A.; Pilkington M. Rational approaches to organic ferromagnets based on neutral radicals appended to organosulfur donors. *Curr. Org. Synth*., **2009**, *6*, 66-78.

54. Coronado, E.; Galan-Mascaros, J. R. Hybrid molecular conductors. *J. Mater. Chem.*, **2005**, *15*, 66-74.
55. Bancerz, M.; Georges, M. K. Verdazyl radicals as substrates for organic synthesis: a synthesis of 3-methyl-5-aryl-1,3,4-oxadiazolones. *J. Org. Chem*., **2011**, *76*, 6377–6382.

56. Milcent, R.; Barbier, G.; Capelle, S.; Catteau, J. P. New general synthesis of tetrahydro-1,2,4,5-tetrazin-3(2H)-one derivatives and stable 3,4-dihydro-3-oxo-1,2,4,5-tetrazin-1(2H)-yl radical derivatives. *J. Heterocycl. Chem*. **1994**, *31*, 319−324.

57. Biltz, H.; Sieden, F. Ueber die oxydation von aldehydphenylhydrazonen zu α-diketonosazonen. *Liebigs Ann. Chem*. **1902**, *324*, 310−328.

58. Jasiński, M.; Gerding, J. S.; Jankowiak, A.; Gębicki, K.; Romański, J.; Jastrzębska, K.; Sivaramamoorthy, A.; Mason, K.; Evans, D. H.; Celeda, M.; Kaszyński, P. Functional group transformations in derivatives of 6-oxoverdazyl. *J. Org. Chem*. **2013**, *78*, 7445−7454.

59. Sase, S.; Jaric, M.; Metzger, A.; Malakhov, V.; Knochel, P. One-pot Negishi cross-coupling reactions of in situ generated zinc reagents with aryl chlorides, bromides, and triflates. *J. Org. Chem*., **2008**, *73*, 7380−7382.

60. Bernhardt, S.; Manolikakes, G.; Kunz, T.; Knochel, P. Preparation of solid salt-stabilized functionalized organozinc compounds and their application to cross-coupling and carbonyl addition reactions. *Angew. Chem. Int. Ed*. **2011**, *50*, 9205 –9209.

61. Batey, R. A.; Shen, M.; Lough, A. J. Carbamoyl-substituted N-heterocyclic carbene complexes of palladium(II): application to sonogashira cross-coupling reactions. *Org. Lett*. **2002**, *4*, 1411-1414.

62. Beingessner, R. L.; Deng B. L.; Fanwick, P. E.; Fenniri, H. A regioselective approach to trisubstituted 2 (or 6)-arylaminopyrimidine-5-carbaldehydes and their application in the synthesis of structurally and electronically unique G-C base precursors. *J. Org. Chem*. **2008**, *73*, 931−939.

63. Fleury-Brégeot, N.; Fleury-Brégeot, N.; Presset, M.; Beaumard, F.; Colombel, V.; Oehlrich, D.; Rombouts, F.; Molander, G. A. Suzuki−Miyaura cross-coupling of potassium alkoxyethyltrifluoroborates: access to aryl/heteroarylethyloxy motifs. *J. Org. Chem*. **2012**, *77*, 10399−10408.

64. Majumdar, K.C.; Ghosha, T.; Chakravorty, S. Synthesis and characterization of symmetrical eight aromatic ring containing bent-shaped material derived from benzophenone. *Mol Cryst Liq Cryst*, **2010** , *533*, 63-72.

65. Bancerz, M.; Georges, M. K. Effects of N1 and N5 alkyl substituents on the stability of 6-oxoverdazyl radicals. *Tetrahedron Letters*, **2012**, *53*, 6846–6848.

66. Jankowiak, A.; Kaszynski, P. Synthesis of oleophilic electron-rich phenylhydrazines. *Beilstein J. Org. Chem*. **2012**, *8*, 275–282.

67. Mohan Reddy, G. S.; Narasimhaswamy, T.; Jayaramudu, J.; Sadiku, E. R.; Raju, K. M.; Ray, S. S. A new series of two-ring-based side chain liquid crystalline polymers: synthesis and mesophase characterization. *Aust. J. Chem*., **2013**, *66*, 667-675.

68. Jakli, A.; Pintre, I. C.; Serrano, J. L.; Ros, M. B.; de la Fuente, M. R. Piezoelectric and electric-field-induced properties of a ferroelectric bent-core liquid crystal. *J. Adv. Mater*. **2009**, *21*, 3784-3788.

69. Naoum, M. M.; Seliger, H.; Happ, E. Effect of structural changes on mesophase stability of some model compounds based on the aryl benzoate group. *Liq. Cryst*. 1997, *23*, 247-253.

70. He, W. L.; Liu, T.; Yang, Z.; Zhao, D. Y.; Huang, W.; Cao, H.; Wang, G. J.; Yang, H. Facile synthesis and characterization of novel thermo-chromism cholesteryl-containing hydrogen-bonded liquid crystals. *Chinese Chem. Lett*., **2009**, *20*, 1303-1306.

71. Genson, K. L.; Holzmueller, J.; Vaknin, D.; Villavicencio, O. F.; McGrath, D. V.; Tsukruk, V. V. Langmuir monolayers from functionalized amphiphiles with epoxy terminal groups. *Thin Solid Films*, 2005, *493*, 237-248.

72. Tao, K.; Wu, T.; Lu, D.; Bai, R.; Li, H.; An, L. Synthesis and characterization of a novel two-component organogelator based on ion-bonded discotic complex. *J. Mol. Liq*. **2008**, *142*, 118-123.